European Journal of Medicinal Chemistry 183 (2019) 111722

Contents lists available at ScienceDirect

European Journal of Medicinal Chemistry

journal homepage: http://www.elsevier.com/locate/ejmech

Research paper

Discovery of novel, potent, isosteviol-based antithrombotic agents

Peng Chen [a], Dianwen Zhang [c], Meng Li [b], Qiong Wu [a], Yuko P.Y. Lam [b], Yan Guo [a], Chen Chen [a], Nan Bai [d, e], Shipra Malhotra [d, f], Wei Li [c], Peter B. O'Connor [b], Hongzheng Fu [a, *]

[a] State Key Laboratory of Natural and Biomimetic Drugs, School of Pharmaceutical Sciences, Peking University, No.38 Xueyuan Road, Haidian District, Beijing, 100191, China
[b] Department of Chemistry, University of Warwick, Gibbet Hill Road, Coventry, CV4 7AL, UK
[c] Academy of Chinese Medical Sciences of Jilin Province, No.155 Chuangju Road, Changchun, 130012, China
[d] Program in Molecular Therapeutics, Fox Chase Cancer Center, 333 Cottman Avenue, Philadelphia, PA, 19111, United States
[e] Department of Molecular Biosciences, University of Kansas, 1200 Sunnyside Avenue, Lawrence, KS, 66045, United States
[f] Center for Computational Biology, University of Kansas, 2030 Becker Drive, Lawrence, KS, 66047, United States

ARTICLE INFO

Article history:
Received 2 July 2019
Received in revised form
18 September 2019
Accepted 19 September 2019
Available online 19 September 2019

ABSTRACT

Thrombosis is a pathological coagulation process and can lead to many serious thrombotic diseases. Here, we report a novel potent antithrombotic compound (**6k**) based on isosteviol with anticoagulant and antiplatelet activities. **6k** selectively inhibited FXa ($K_i = 0.015$ μM) against a panel of serine proteases and showed excellent anticoagulant activity (significant prolongation of ex vivo PT and aPTT over the vehicle, $p < 0.01$). **6k** also significantly inhibited ADP-induced platelet aggregation in rats relative to the vehicle ($p < 0.01$). Furthermore, **6k** exhibited potent ex vivo and in vivo antithrombotic activity in rats relative to the vehicle ($p < 0.01$ and $p < 0.0001$, respectively). Novel structure **6k**, with potent antithrombotic activity, is expected to lead a promising approach for the development of antithrombotic agents.

1. Introduction

In contemporary society, thromboembolic disorders such as stroke (arising from atrial fibrillation), unstable angina, myocardial infarction, and venous thromboembolism (VTE) are linked to significant increases in mortality and morbidity [1–3]. Thrombus formation involves the coagulation cascade and platelet activation. Therefore, clinical antithrombotic therapy mainly use anticoagulant and antiplatelet agents [4].

The platelet activating receptors, such as thromboxane A2 (TXA2) receptor, protease-activated receptor-1 (PAR-1), and adenosine diphosphate (ADP) receptors, on the platelet surface play an important role in platelet activation, aggregation, and adherence to the vessel wall [5]. Currently, antiplatelet agents target these specific receptors to prevent clot formation. Although antiplatelet agents serve as important treatments for thrombosis, they often cause side effects, such as increased risk of recurrent thrombosis caused by insufficient therapy intensity [6], gastrointestinal ulcers and bleeding [7] and thrombotic thrombocytopenic purpura [8]. Thus, further development of novel antiplatelet agent is still urgent for thrombotic therapies.

Anticoagulation therapy is central to the management of thromboembolic diseases. Although several anticoagulants, such as fondaparinux, warfarin, low-molecular-weight heparins and unfractionated heparin, are effective in the prevention and treatment of these thrombotic diseases, they have several undesirable effects [9–11]. Recent research has shown that factor IIa (FIIa) and factor Xa (FXa) are promising targets for the development of potent, selective, and orally bioavailable anticoagulants [12]. FXa is located at the junction of the intrinsic and extrinsic pathways of coagulation, and it catalyzes the conversion of prothrombin to thrombin. Unlike thrombin inhibitors, selective FXa inhibitors reduce further generation of thrombin while having a smaller effect on existing thrombin levels, which may in turn decrease the risk of bleeding, providing a more favorable safety profile [13]. Currently available novel FXa inhibitors, rivaroxaban [14], apixaban [15], betrixaban [16] and edoxaban [17], show advantages over traditional anticoagulants [18]. However, they still have many drawbacks such as

Abbreviations: FXa, factor Xa; FIIa, factor IIa; FXIa, factor XIa; FVIIa, factor VIIa; FXIIa, factor XIIa; FIXa, factor IXa; PK, plasma kallikrein; PT, prothrombin time; aPTT, activated partial thromboplastin time; TLC, thin-layer chromatography.

* Corresponding author.
E-mail address: drhzfu@gmail.com (H. Fu).

https://doi.org/10.1016/j.ejmech.2019.111722
0223-5234/

narrow clinical indications [19,20], long half-lives [21,22], bleeding risks [23], and unwanted drug to drug interactions [24]. Therefore, further development of FXa inhibitors with novel structures is still required for thrombotic diseases.

In recent years, compounds containing anticoagulant and antiplatelet activity have been considered novel promising antithrombotic agents [25–30] due to their potent antithrombotic activity, low risk of drug-drug interactions and less demanding clinical studies [31,32].

Natural products have historically been a rich source for successful drugs, and represent an important pool for the identification of new pharmacological leads today [33]. Given their core scaffolds with specific stereochemistry, related modified structures may possess potent bioactivities. Therefore, the modification of molecules derived from natural products to obtain novel bioactive compounds has attracted significant attention [34–39].

Isosteviol (Fig. 1), a tetracyclic diterpenoid with a beyerane scaffold, is obtained by the acid hydrolysis of naturally abundant stevioside [40]. Due to its relatively low toxicity, low cost, rigidity, and chiral framework, it has been noted for its extensive bioactivity [41]. Although isosteviol has not been reported to possess antithrombotic activity, its tetracyclic diterpenoid skeleton was found to possess anticoagulant and antiplatelet activities [42,43], and this inspired our investigation of this structure to develop novel and potent antithrombotic agent [44].

We describe a novel potent antithrombotic compound (**6k**) based on isosteviol through empirical medicinal chemistry strategy. The strategy facilitated to discover novel, potent antithrombotic compounds efficiently and economically. The in vitro biological investigations and pharmacology studies on rats provided evidence that the novel structure possessed potent antithrombotic activity.

2. Results and discussion

Lead compound discovery. Preliminary large-scale synthesis of reported isosteviol derivatives was conducted to find possible lead compounds by evaluating their in vitro anticoagulant activity and in vivo antithrombotic activity. To obtain compounds easily and economically, we chose one-pot reactions with moderate conditions that provided high yields and synthesized **2**–**6** [45–47]. Initial synthetic efforts were focused on the C-16 carbonyl and C-19 carboxyl positions of isosteviol. The in vitro activities of **1**–**6** against human FXa showed that **6** ($K_i = 2.7$ μM) exhibited a relatively better inhibitory activity (Fig. 1a). The results also indicated that the 19-ethyl ester group may enhance the anticoagulant activity based on the results of **2** ($K_i = 4.6$ μM) and **1** ($K_i = 13.4$ μM) and the results of **6** and **5** ($K_i = 8.0$ μM); the 16-oxime group may also improve anticoagulant efficacy based on comparisons of **5** and **1** or **6** and **2**. The effects of **1**–**6** on in vivo thrombus formation time in rats were also investigated to confirm their antithrombotic activity. Although the efficacy of **6** was not as good as clinical drugs, it caused significant prolongation of thrombus formation time with a better efficacy than **1**–**5** (Fig. 1b). Therefore, **6** was considered to be the lead compound, and it was subjected to further modifications to improve its anticoagulant activity.

Modification of the lead compound and in vitro FXa inhibition evaluation. Preliminary lead compound screening helped us identify that the 19-ethyl ester group and the 16-oxime group of lead compound **6** were key to the anticoagulant activity. To find potent anticoagulant candidates, we synthesized a series of oxime ether derivatives (Scheme 1) through functional group [48,49] conversions of the 16-oxime group as oxime ethers have been noted for their potent anticoagulant bioactivity [50], and the in vitro activity against human FXa of these derivatives were evaluated.

The in vitro bioactivities of the collection indicated that oxime ether derivatives containing a thiophene group (**6k**, $K_i = 0.015$ μM) or a 3-methyloxetane group (**6p**, $K_i = 0.028$ μM) showed excellent in vitro efficacies against human FXa (Table 1) with activities more than 95-fold better than that of lead compound **6** ($K_i = 2.7$ μM). The inhibition efficacies of **6a-g** indicated that of the tested substituted benzene groups, a pentafluorobenzene group (**6g**, $K_i = 0.321$ μM) can enhance activity. The in vitro inhibitory activities of **6ra-rt** (Table 2) indicated that derivatives containing π-π conjugated aromatic-alkenyl groups did not offer significantly enhanced efficacy. **6rm** ($K_i = 0.211$ μM) showed slight inhibition efficacy, indicating that the inserted π-π conjugate phenyl-alkenyl group may reduce the inhibitory efficacy against human FXa relative to that of **6k**. In general, **6g** and **6rm** showed relatively low potencies against human FXa.

Selectivity against a panel of serine proteases. In addition, we found that **6k** and **6p** selectively inhibited FXa against a panel of serine proteases in the coagulation pathway (Table 3). **6k** showed excellent selectivity against a panel of human serine proteases with K_i values less than 5 μM for FXIa, PK, the digestive enzyme trypsin, and the fibrinolytic enzymes tPA and uPA (80-300-fold selectivity) and K_i values greater than 5 μM for FVIIa, FXIIa, FIXa and

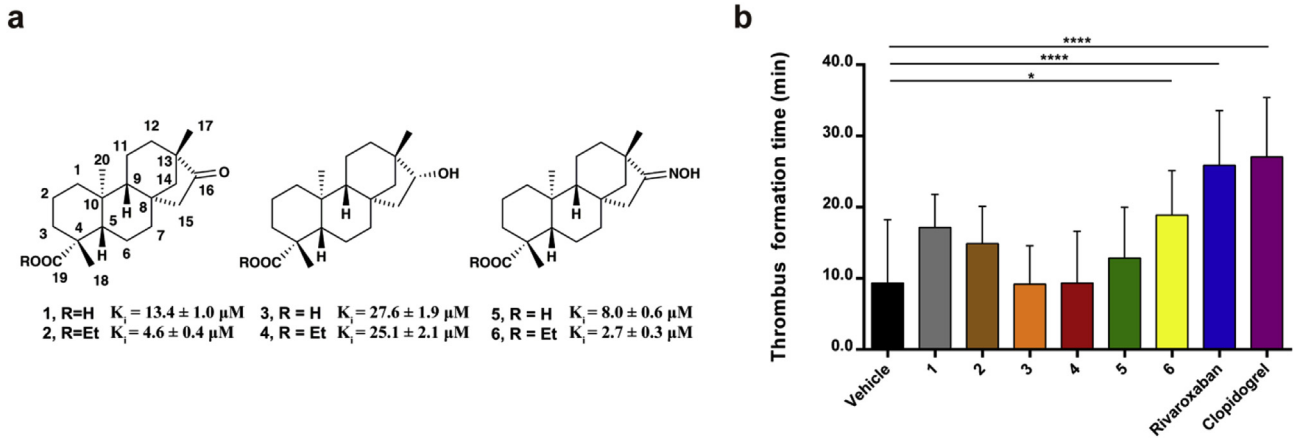

Fig. 1. Preliminary evaluation of the reported compounds. (a) In vitro anticoagulant activities of the reported structures. Values are presented as the mean ± SD (n = 5). (b) In vivo antithrombotic efficacies were evaluated in a rat electric-stimulated arterial thrombosis model after an oral dose of 22 μmol/kg. Values are presented as the mean ± SD (n = 8). Statistical significance of the difference relative to the vehicle group was analyzed by one-way ANOVA with Dunnett's multiple comparison test: $^{*}p < 0.05$, $^{****}p < 0.0001$.

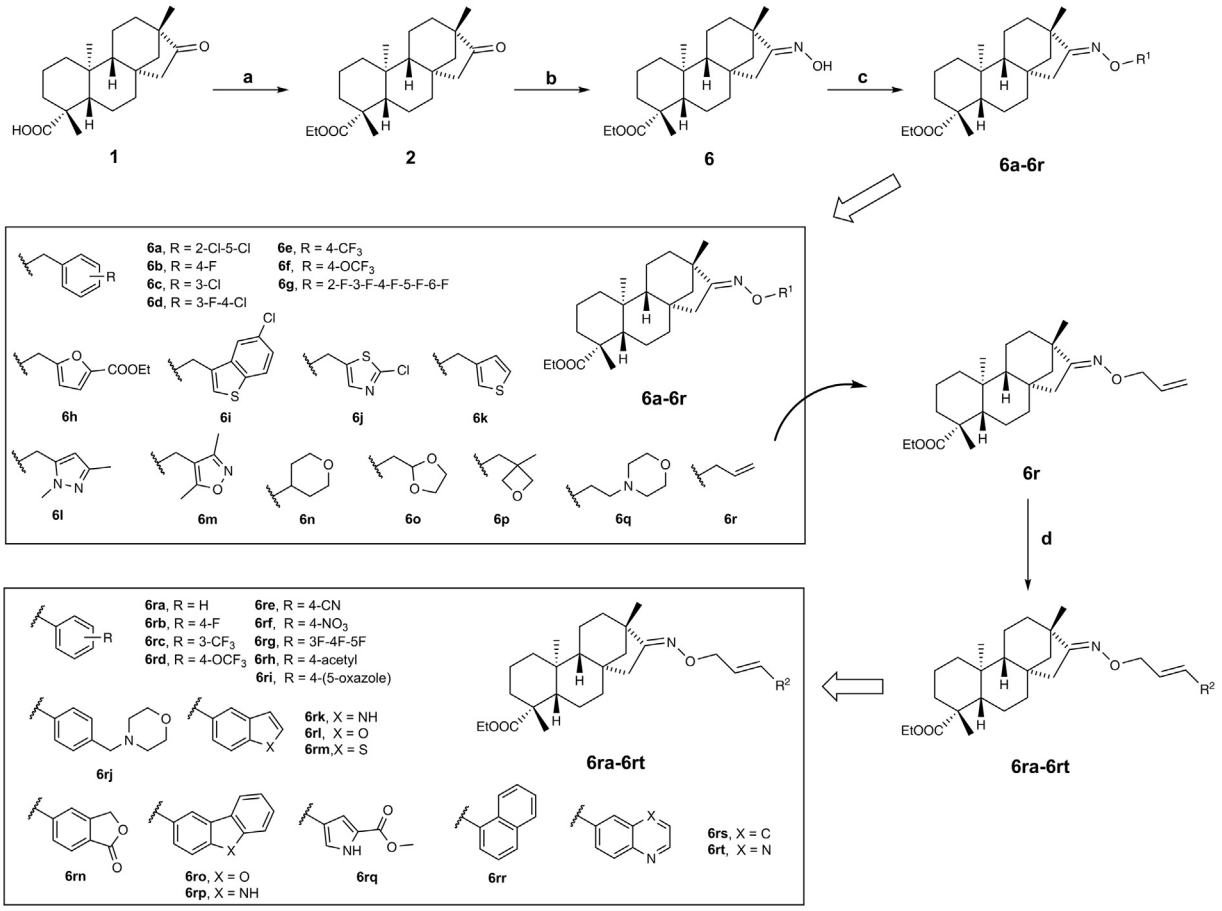

Scheme 1. Synthesis of Isosteviol Derivatives.[a]

[a] Reagents and conditions: (a) EtBr, KOH, DMSO, 25 °C, 4 h; (b) $NH_2OH{\cdot}HCl$, $NaHCO_3$, EtOH, 60 °C, 2 h; (c) NaH, R^1X, DMF, 0 °C. X = Cl, Br; (d) 10% mmol $Pd(OAc)_2$, 20% mmol P(O-Tolyl)$_3$, R^2X, Et_3N, ACN, 40 °C. R^2X represents (hetero)aryl halides, X = Br, I.

chymotrypsin (>500-fold selectivity). **6p** slightly less specific on human serine protease, as it showed less than 20-fold selectivity for PK and trypsin. In general, **6k** exhibited better selectivity than **6p** against a panel of serine proteases. The high selectivity of **6k** will help ensure efficient anticoagulant activity and a suitable safety profile.

Docking study. Furthermore, to elucidate the binding mode of **6k** and **6p** to FXa, we conducted docking studies using AutoDock Vina [51]. The criteria for choosing the model were a good fit and good interactions, such as hydrogen bonds and interaction energies. The protein human factor Xa has been solved with different ligands. Although the ligands have different chemical structures and have different solved binding poses, the protein conformation remains stable. Thus, we docked **6k** and **6p** in protein human factor Xa and found models for **6k** and **6p** that looked promising for ligand binding (Fig. 2). The binding model of **6k** indicated that the thiophene moiety and the oxime moiety occupied the S1 pocket, while the fused polycyclic hydrocarbon moiety of the core scaffold and the ethyl ester moiety fit in the S4 pocket formed by the residues Phe174, Trp215, and Tyr99. The thiophene moiety of **6k** interacts with the aromatic ring of Tyr228 located at the bottom of the S1 pocket. Hydrogen bonding was observed between the nitrogen of C-16 (**6k**) and the carbonyl group of Gln192 (FXa), and between the oxygen at C-23 (**6k**) and the NH of Gln192 (FXa). The binding model of **6p** showed similar interactions in S1 and S4 pockets. The 3-methyloxetane moiety of **6p** interacts with the aromatic ring of Tyr228 located at the bottom of the S1 pocket. Hydrogen bonding was observed between the nitrogen at C-16 (**6p**) and the carbonyl group of Gln192 (FXa) and between the oxygen at C-19 (**6p**) and the NH of Trp215 (FXa). The models of both **6k** and **6p** exhibit excellent interactions and fit based on the binding affinities.

Pharmacokinetic study. The pharmacokinetic parameters (Table 4) of **6k** and **6p** in rats showed no apparent disadvantage; **6k** exhibited better oral maximal plasma concentration (C_{max} = 1245.6 μg/l) and a higher plasma exposure ($AUC_{0\sim\infty}$ = 5528.9 μg h/L) than **6p** (C_{max} = 728.5 μg/L, $AUC_{0\sim\infty}$ = 4811.7 μg h/L). The oral bioavailability of **6k** (48.6%) was also better than **6p** (42.7%).

Ex vivo anticoagulant activity. In addition, we assessed the anticoagulant activities of **6k** and **6p** through ex vivo PT and aPTT assays (Fig. 3). The ex vivo PT and aPTT assays were conducted using rat plasma after a dose of 22 μmol/kg by oral gavage. **6k** ($^{**}p < 0.01$) significantly prolonged PT and showed better prolongation than **6p**. **6k** ($^{**}p < 0.01$) also significantly prolonged aPTT and showed better prolongation than **6p** ($^{*}p < 0.05$). In general, **6k** ($^{**}p < 0.01$) exhibited significant prolongation in ex vivo PT and aPTT assays.

Ex vivo antiplatelet aggregation. Furthermore, **6k** and **6p** were evaluated for their inhibitory effects on ADP-induced platelet aggregation in rats at a dose of 22 μmol/kg (Fig. 4). **6k** ($^{**}p < 0.01$) was found to have a similar inhibition efficacy as that of the positive control (clopidogrel) on platelet aggregation [52]. Although **6p** ($^{*}p < 0.05$) significantly reduced the platelet aggregation rate compared with the vehicle, it was less potent than **6k**.

Ex vivo and in vivo antithrombotic activity. To evaluate the

Table 1
FXa inhibitory effect of compound 6a-6r.

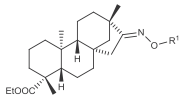

Compd.	r^1	K_i (μM) [a]	Compd.	r^1	K_i (μM)
6a	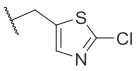	9.253 ± 0.728	**6j**	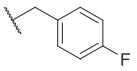	1.941 ± 0.149
6b	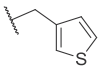	4.333 ± 0.457	**6k**	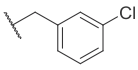	0.015 ± 0.002
6c	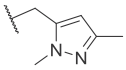	18.087 ± 1.463	**6l**	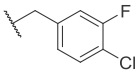	4.025 ± 0.312
6d	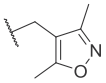	9.786 ± 0.769	**6m**	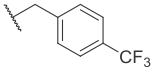	2.875 ± 0.213
6e		2.693 ± 0.356	**6n**	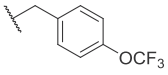	1.809 ± 0.207
6f	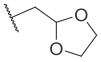	1.023 ± 0.114	**6o**	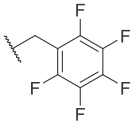	1.612 ± 0.104
6g		0.321 ± 0.039	**6p**	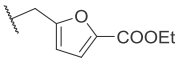	0.028 ± 0.002
6h	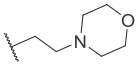	9.877 ± 0.922	**6q**	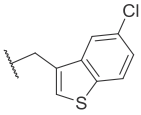	0.785 ± 0.058
6i		0.515 ± 0.049	**6r**	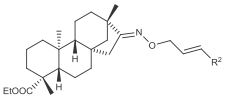	8.607 ± 0.837

[a] Values are presented as the mean ± SD (n = 5).

antithrombotic activities of **6k** and **6p**, we compared the efficacies of **6k**, **6p** and antithrombotic drugs in ex vivo and in vivo antithrombotic assays on rats at the same oral gavage dose (22 μmol/kg). The ex vivo antithrombotic efficacies of **6k** and **6p** were determined based on their effects on the thrombogenesis model using the Chandler method [53]. The results of the ex vivo antithrombotic assay were evaluated through wet weight and dry weight of thrombus (Fig. 5). **6k** and **6p** significantly reduced the wet weight and dry weight of thrombus. **6k** ($^{**}p < 0.01$) showed higher ex vivo antithrombotic activity than **6p** ($^{*}p < 0.05$), rivaroxaban ($^{*}p < 0.05$) and clopidogrel ($^{*}p < 0.05$).

In addition, in vivo antithrombotic activity was carried out to observe their effects on thrombogenesis in rats at the same dose (22 μmol/kg) by oral gavage. Electrical stimulation of the common carotid artery [54] was adopted to form in vivo thrombosis (Fig. 6). The analysis of the in vivo antithrombotic efficacies showed that both **6k** and **6p** significantly prolonged the thrombus formation time in rats. **6k** ($^{****}p < 0.0001$) showed better in vivo antithrombotic activity than **6p** ($^{**}p < 0.01$), rivaroxaban ($^{***}p < 0.001$) and clopidogrel ($^{**}p < 0.01$). In general, **6k** exhibited potent antithrombotic activity.

3. Conclusion

To summarize, using a medicinal chemistry strategy, we found a novel oxime ether containing a thiophene group (**6k**) with a core scaffold based on isosteviol (a natural product), and this compound possesses potent antithrombotic activity. We selected compound **6** as the lead compound based on the evaluations of both in vitro anticoagulant and in vivo antithrombotic efficacies of reported modification derivatives. A collection of isosteviol derivatives based on lead compound **6** were synthesized, and their in vitro inhibitory activities against FXa were evaluated, from which, we found two potent anticoagulant compounds **6k** and **6p**. We also discovered that **6k** and **6p** selectively inhibited FXa against a panel of serine proteases, and **6k** showed better selectivity than **6p**. Ex vivo anticoagulant evaluations using PT and aPTT assays demonstrated that **6k** exhibited anticoagulant activity and was more effective than **6p**. **6k** also showed better inhibitory efficacy on ADP-induced platelet aggregation than **6p**. The potent activity of **6k** in ex vivo and in vivo antithrombotic assays demonstrated that **6k**, a novel scaffold possessing anticoagulant and antiplatelet activities, is a promising antithrombotic agent. This unique scaffold based on isosteviol will facilitate the exploration of novel antithrombotic agents.

Table 2
FXa inhibitory effect of compound 6ra-6rt.

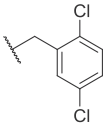

Compd.	r^2	K_i (μM) [a]	Compd.	r^2	K_i (μM)
6ra		10.697 ± 1.003	**6rk**	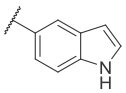	4.674 ± 0.431
6rb	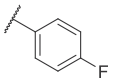	6.169 ± 0.579	**6rl**	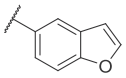	10.276 ± 0.973
6rc	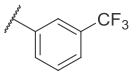	4.861 ± 0.427	**6rm**	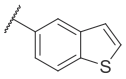	0.211 ± 0.020
6rd	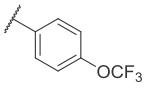	1.974 ± 0.127	**6rn**	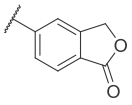	20.671 ± 2.312
6re	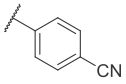	13.342 ± 1.210	**6ro**	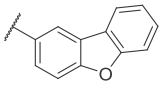	20.984 ± 2.026
6rf	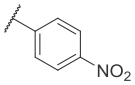	2.636 ± 0.256	**6rp**	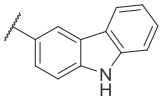	26.433 ± 3.169
6rg	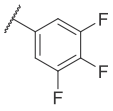	1.980 ± 0.143	**6rq**	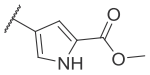	1.913 ± 0.164
6rh	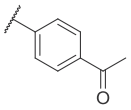	1.643 ± 0.153	**6rr**	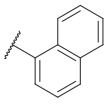	12.136 ± 1.353
6ri	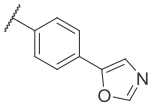	1.931 ± 0.162	**6rs**	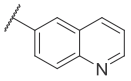	4.177 ± 0.381
6rj	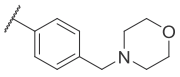	2.492 ± 0.210	**6rt**	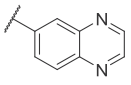	3.603 ± 0.342
rivaroxaban		3.4 ± 0.4 (nM)			

[a] Values are presented as the mean ± SD (n = 5).

Table 3
In vitro selectivity profile against a panel of serine proteases.

Compd.	K_i (μM) [a]								
	FXIa	FVIIa	FXIIa	FIXa	PK	trypsin	chymotrypsin	tPA	uPA
6k	1.7 ± 0.2	11.6 ± 1.2	9.3 ± 1.0	19.7 ± 2.3	2.2 ± 0.3	2.1 ± 0.2	16.3 ± 1.7	3.5 ± 0.2	4.4 ± 0.1
6p	1.9 ± 0.1	8.0 ± 0.9	7.6 ± 0.7	4.8 ± 0.5	0.3 ± 0.1	0.3 ± 0.1	12.4 ± 1.6	2.8 ± 0.4	2.0 ± 0.2

[a] Data are presented as the mean ± SD (n = 5).

4. Experimental section

General Procedures. ^{1}H NMR, ^{19}F NMR and ^{13}C NMR data were recorded on a Bruker Avance III 400 spectrometer (Bruker, Karlsruhe, Baden−Wuerttemberg, Germany). Chemical shifts are reported in parts per million (ppm) using the following internal references: ^{1}H, δ 7.26 for $CDCl_3$, 3.31 for CD_3OD; ^{13}C, δ 77.0 for $CDCl_3$, 49.0 for CD_3OD. Signal multiplicities are recorded as singlet (s),

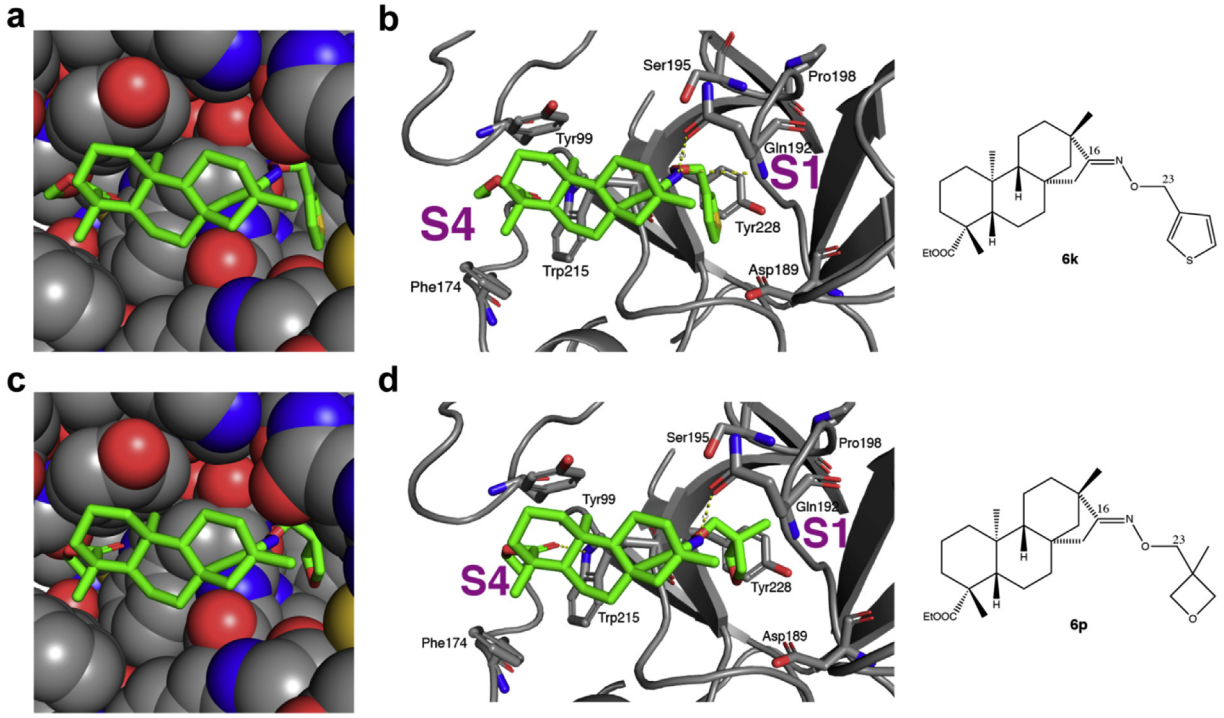

Fig. 2. Docking models of **6k** (a, b) and **6p** (c, d) with the binding sites of human FXa (PDBID: 2W26); the protein is shown in salmon, and the molecules are shown in green. (a), (c), Spheres form of the docking model. (b), (d), Cartoon form of the docking model and 2D structures of **6k** and **6p**; the essential amino acids are drawn as sticks, and the hydrogen bonds are shown as yellow dotted lines. (For interpretation of the references to colour in this figure legend, the reader is referred to the Web version of this article.)

Table 4
Pharmacokinetic data for 6k and 6p in rats.

Compd.	Route	C_{max} (μg/L)	$t_{1/2}$ (h)	$AUC_{0-\infty}$	MRT (h)	CL (L/h)	V (L)	F (%)
6k	p.o.[a]	1245.6 ± 94.9	3.9 ± 0.1	5528.9 ± 246.4	4.1 ± 0.1	1.8 ± 0.1	10.2 ± 0.5	48.6
	i.v.[b]		3.2 ± 0.1	3409.4 ± 230.1	4.6 ± 0.1	0.9 ± 0.1	4.0 ± 0.4	
6p	p.o.	728.5 ± 52.7	4.2 ± 0.1	4811.7 ± 136.7	5.6 ± 0.2	2.1 ± 0.1	12.5 ± 0.5	42.7
	i.v.		3.4 ± 0.1	3381.7 ± 255.6	4.9 ± 0.2	0.9 ± 0.1	4.3 ± 0.5	
rivaroxaban	p.o.	1577.0 ± 267.8	3.7 ± 0.2	6984.9 ± 1611.9	5.4 ± 0.3	1.5 ± 0.3	8.1 ± 2.0	59.7
	i.v.		4.4 ± 0.2	3508.7 ± 592.0	6.3 ± 0.3	0.9 ± 0.1	5.5 ± 0.8	

[a] Given p.o. at 22 μmol/kg.
[b] Given i.v. at 6.6 μmol/kg.

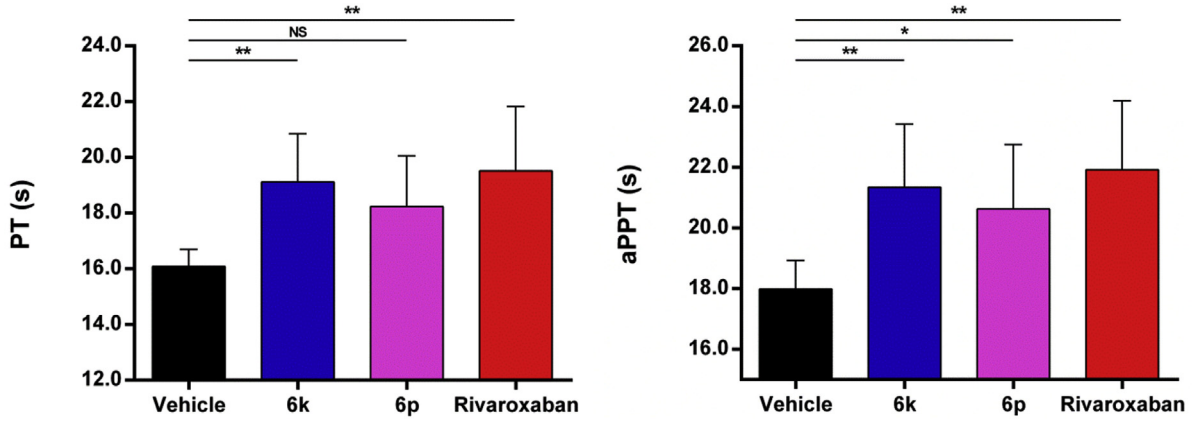

Fig. 3. The results of the ex vivo PT and aPTT assays are given as a prolongation percentage after an oral dose of 22 μmol/kg. Values are presented as the mean (n = 8). Each data represents the measured value from an individual rat in the test group. Statistical significance of the difference in comparison with the vehicle group was analyzed by one-way ANOVA with Dunnett's multiple comparison test: $^{*}p < 0.05$, $^{**}p < 0.01$, NS = nonsignificant.

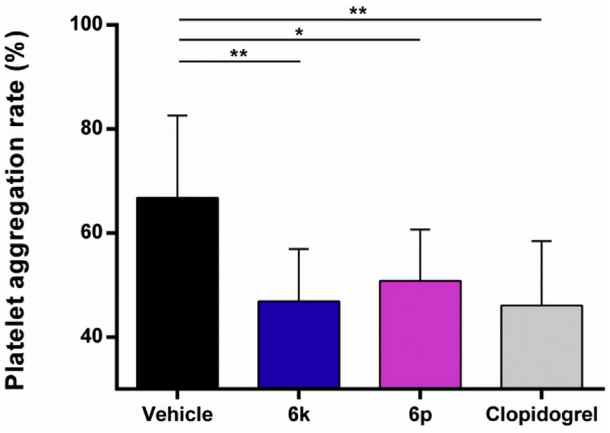

Fig. 4. Ex vivo inhibition of platelet aggregation in rats after an oral dose of 22 μmol/kg. Values are presented as the mean ± SD (n = 8). Each data point represents the measured value from an individual rat in the test group. Statistical significance of the differences relative to the vehicle group were analyzed by one-way ANOVA with Dunnett's multiple comparison test: $^{*}p < 0.05$, $^{**}p < 0.01$, NS = nonsignificant.

doublet (d), triplet (t), quartet (q), multiplet (m), doublet of doublets (dd), triplet of doublets (td). Coupling constants (*J*) are reported to the nearest 0.1 Hz. Spectra were analyzed using Bruker TopSpin 2.1 software. Unless otherwise stated, all reactions were carried out in oven-dried glassware under an inert atmosphere of argon with dry solvents, all solvents were obtained from commercial sources and were purified according to standard procedures, and all commercially obtained reagents were used as received. Products were purified by column chromatography using silica gel (200–300 mesh, Qingdao Marine Chemical Factory, Qingdao, China). Thin-layer chromatography (TLC) separation were performed on Merck silica gel GF254 plates and visualized with UV light (254 nm). Melting points were measured on a melting point apparatus (M – 560, Buchi). Infrared (IR) spectra were recorded as KBr disks on a Nicolet 470 FT-IR spectrophotometer (Nicolet, Madison, WI, USA). High-resolution mass spectrometry (HRMS) data were recorded on a Waters Xevo G2 Q-TOF mass spectrometer. The purity of each compound was determined on a Waters Alliance e2695 HPLC. All compounds were >95% purity by HPLC analysis, and the purities of **6k** and **6p** were >99% (for pharmacological studies). Ultrahigh resolution mass spectrometry fragmentation characterizations of **6k** and **6p** using Fourier transform ion cyclotron resonance mass spectrometer (FT-ICR MS) were conducted on a 12 T SolariX (Bruker Dlatonik GmbH, Bremen, Germany).

(4R,4aS,6aR,9S,11aR,11bS)-4,9,11b-trimethyl-8-oxotetradecahydro-6a,9-methanocyclohepta[a]naphthalene-4-carboxylic acid (1). To a solution of stevioside (402.4 g, 0.5 mol) in MeOH–H_2O (4:1, 1000 mL) was added H_2SO_4 (250 mL, 3 M). The mixture was heated to reflux and stirred for 8 h and then concentrated under vacuum to remove most of the MeOH. The mixture was filtered through a Büchner funnel, and the obtained solid was washed with water and recrystallized. Isosteviol (**1**, 149.5 g, 94%) was obtained by recrystallization from $CHCl_3$–MeOH (2:1) at room temperature, m.p. 232.0–232.6 °C; X-ray crystal data can be obtained from the Cambridge Crystallographic Data Centre: CCDC 1577011; IR (KBr): 3474, 2989, 2946, 2894, 1702, 1649, 1452, 1252, 1187, 1056 cm^{-1}; ^{1}H NMR (400 MHz, $CDCl_3$): δ 2.65 (dd, $J = 3.7$, 18.6 Hz, 1H), 2.18 (d, $J = 13.5$ Hz, 1H), 1.31–1.95 (m, 13H), 1.26 (s, 3H), 1.13–1.25 (m, 3H), 1.0–1.09 (m, 1H), 0.99 (s, 3H), 0.87–0.97 (m, 1H), 0.79 (s, 3H); ^{13}C NMR (100 MHz, $CDCl_3$): δ 222.8, 183.9, 57.0, 54.7, 54.3, 48.7, 48.4, 43.7, 41.4, 39.7, 39.5, 38.2, 37.6, 37.3, 29.0, 21.6, 20.3, 19.8, 18.9, 13.3; HRMS (ESI, *m/z*) calculated for $C_{20}H_{31}O_3$ $[M+H]^+$: 319.2273; found: 319.2274.

Ethyl (4R,4aS,6aR,9S,11aR,11bS)-4,9,11b-trimethyl-8-oxotetradecahydro-6a,9-methanocyclohepta[a]naphthalene-4-carboxylate (2). To a solution of isosteviol (**1**, 31.8 g, 0.1 mol) in DMSO (100 mL) was added EtBr (16.3 g, 11.2 mL, 0.15 mol) and KOH (8.4 g, 0.15 mol) at 25 °C. After stirring for 4h, the mixture was added into 1000 mL of ice water to precipitate a white powder. Then, the mixture was filtered through a Büchner funnel, and the obtained white powder was washed with water and recrystallized from EtOH to afford **2** as colorless crystals (33.3 g, 96%), m.p. 122.2–122.8 °C; X-ray crystal data can be obtained from the Cambridge Crystallographic Data Centre: CCDC 1577012; IR (KBr): 2956, 2928, 2845, 1728, 1465, 1380, 1227, 1151, 1095, 1026 cm^{-1}; ^{1}H NMR (400 MHz, $CDCl_3$): δ 4.11 (q, $J = 7.0$ Hz, 2H),2.65 (dd, $J = 18.5$, 3.2 Hz, 1H), 2.19 (d, $J = 13.3$ Hz, 1H), 2.04–1.33 (m, 14H), 1.27 (t, $J = 7.1$ Hz, 3H), 1.23–1.21 (m, 1H), 1.2 (s, 3H), 1.16–1.0 (m, 2H), 0.99 (s, 3H), 0.97–0.86 (m, 1H), 0.73 (s, 3H); ^{13}C NMR (100 MHz, $CDCl_3$): δ 222.5, 177.3, 60.0, 57.0, 54.7, 54.3, 48.7, 48.5, 43.7, 41.6, 39.9, 39.5, 38.0, 37.9, 37.3, 28.9, 21.7, 20.3, 19.9, 19.0, 14.1, 13.4; HRMS (ESI, *m/z*) calculated for $C_{22}H_{35}O_3$ $[M+H]+$: 347.2586; found: 347.2575.

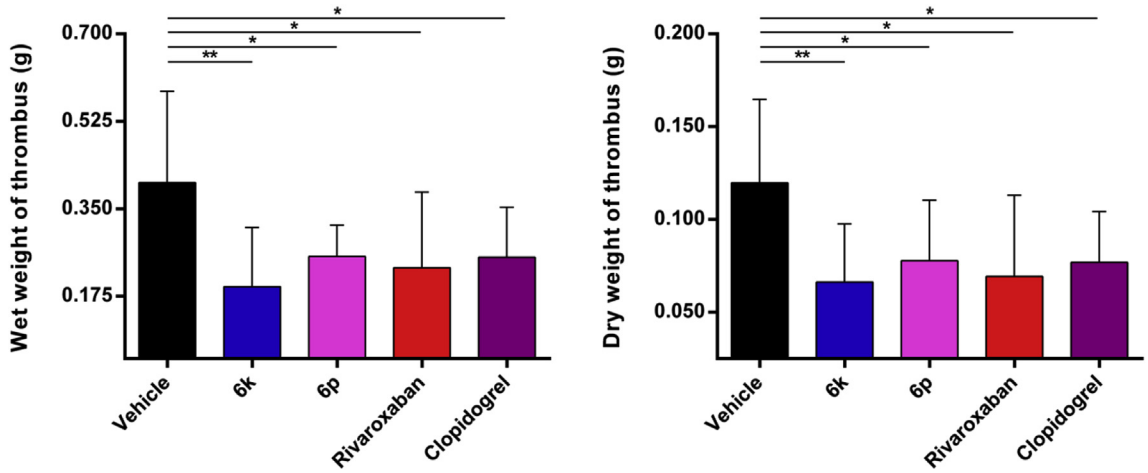

Fig. 5. Ex vivo antithrombotic efficacies on rats after an oral dose of 22 μmol/kg. Values are presented as the mean ± SD (n = 10). Each data point represents the measured value from an individual rat in the test group. Statistical significance of the difference in comparison with the vehicle group was analyzed by one-way ANOVA with Dunnett's multiple comparison test: $^{*}p < 0.05$, $^{**}p < 0.01$.

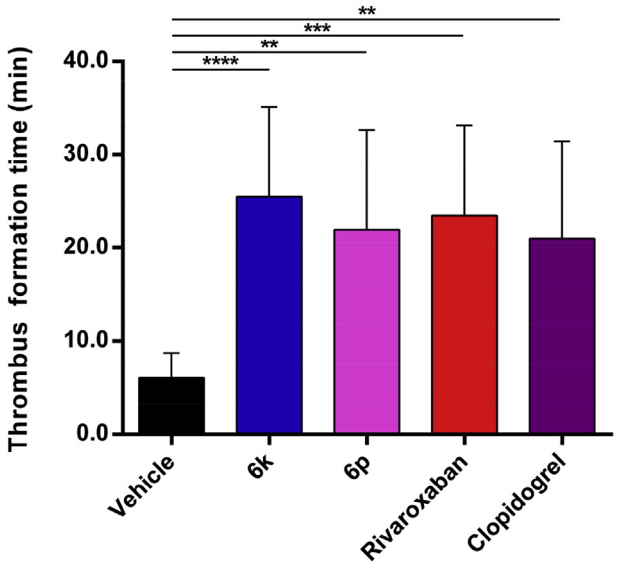

Fig. 6. In vivo antithrombotic efficacies on rats after an oral dose of 22 μmol/kg. Data are presented as the mean ± SD (n = 10). Statistical significance of the difference in comparison with the vehicle group was analyzed by one-way ANOVA with Dunnett's multiple comparison test: $^{**}p < 0.01$, $^{***}p < 0.001$, $^{****}p < 0.0001$.

(4R,4aS,6aR,8R,9S,11aR,11bS)-8-hydroxy-4,9,11b-trimethyltetradecahydro-6a,9-methanocyclohepta[a]naphthalene-4-carboxylic acid (3). To a solution of isosteviol **1** (31.8 g, 0.1 mol) in EtOH (200 mL) was added $NaBH_4$ (5.7 g, 0.15 mol) slowly at 0 °C. The mixture was stirred for 2 h. Then mixture was quenched with a saturated NH_4Cl aqueous solution. After that, the reaction mixture was concentrated under vacuum, and extracted with CH_2Cl_2 and H_2O. The organic layer was washed with saturated NaCl aqueous solution, dried with $MgSO_4$ and concentrated under vacuum to give white powder, then recrystallized from EtOH–H_2O (1:1) to afford compound **3** as a colourless crystal (30.1 g, 94%), m.p. 188.6–190.5 °C; X-ray crystal file is available from the Cambridge Crystallographic Data Centre: CCDC 1577013; IR (KBr): 3474, 2989, 2946, 2894, 1702, 1649, 1452, 1252, 1187, 1056 cm^{-1}; ^1H NMR (400 MHz, CD_3OD): δ 3.78 (dd, $J = 4.4$ Hz, 1H), 2.10 (d, $J = 13.1$ Hz, 1H), 1.20–1.95 (m, 14H), 1.16 (s, 3H), 0.92–1.14 (m, 5H), 0.88 (s, 3H), 0.85 (s, 3H); ^{13}C NMR (100 MHz, CD_3OD): δ 181.7, 81.0, 58.4, 57.4, 56.6, 44.6, 43.6, 43.2, 43.1, 43.0, 41.3, 39.3, 39.2, 35.0, 29.6, 25.4, 23.0, 21.4, 20.1, 14.0; HRMS (ESI, *m/z*) calculated for $C_{20}H_{31}O_3$ $[M-H]^-$: 319.2273; found: 319.2274.

Ethyl (4R,4aS,6aR,8R,9S,11aR,11bS)-8-hydroxy-4,9,11b-trimethyltetradecahydro-6a,9-methanocyclohepta[a]naphthalene-4-carboxylate (4). To a solution of compound **2** (34.6 g, 0.1 mol) in EtOH (200 mL) was added $NaBH_4$ (5.7 g, 0.15 mol) slowly at 0 °C. The mixture was stirred for 2 h. Then mixture was quenched with a saturated NH_4Cl aqueous solution. After that the reaction mixture was concentrated under vacuum, and extracted with CH_2Cl_2 and H_2O. The organic layer was washed with saturated NaCl aqueous solution, dried with $MgSO_4$ and concentrated under vacuum to give white powder, then recrystallized from EtOH to afford compound **4** as a colourless crystal (33.0 g, 95%), m.p. 152.9–153.6 °C; X-ray crystal file is available from the Cambridge Crystallographic Data Centre: CCDC 1554564; IR (KBr): 3533, 2981, 2940, 2837, 1700, 1454, 1230, 1178, 1151, 1047 cm^{-1}; ^1H NMR (400 MHz, $CDCl_3$): δ 4.10 (t, $J = 7.2$ Hz, 2H), 3.87 (dd, $J = 4.8$, 10.6 Hz, 1H), 2.18 (d, $J = 13.6$ Hz, 1H), 1.29–1.89 (m, 14H), 1.27 (t, $J = 7.1$ Hz, 3H), 1.18 (s, 3H), 0.95–1.09 (m, 4H), 0.93 (s, 3H), 0.83–0.91 (m, 1H), 0.77 (s, 3H); ^{13}C NMR (100 MHz, $CDCl_3$): δ 177.6, 80.6, 59.9, 57.2, 55.8, 55.2, 43.7, 42.8, 42.1, 42.0, 41.8, 40.0, 38.1, 38.0, 33.7, 29.0, 24.9, 21.8, 20.5, 19.0, 14.1, 13.4; HRMS (ESI, *m/z*) calculated for $C_{22}H_{37}O_3$ $[M+H]^+$: 349.2743; found: 349.2743.

(4R,4aS,6aR,9S,11aR,11bS,E)-8-(hydroxyimino)-4,9,11b-trimethyltetradecahydro-6a,9-methanocyclohepta[a]naphthalene-4-carboxylic acid (5). To a solution of isosteviol **1** (31.8 g, 0.1 mol) in EtOH (200 mL) was added $NH_2OH{\cdot}HCl$ (10.4 g, 0.15 mol) and $NaHCO_3$ (12.6 g, 0.15 mol). The mixture was stirred at 60 °C for 2 h. The mixture was then concentrated under vacuum, and extracted with CH_2Cl_2 and H_2O. The organic layer was washed with saturated NaCl aqueous solution, dried with $MgSO_4$ and concentrated under vacuum to give white powder **5** (30.6 g, 92%); IR (KBr): 3287, 2941, 2848, 1693, 1671, 1454, 1263, 1190, 1031 cm^{-1}; ^1H NMR (400 MHz, $CDCl_3$): δ 2.4 (dd, $J = 2.4$, 18.8 Hz, 1H), 2.19 (d, $J = 13.2$ Hz, 1H), 2.02 (d, $J = 18.8$ Hz, 1H), 1.27–1.97 (m, 13H), 1.25 (s, 3H), 1.18–1.24 (m, 1H), 1.12 (s, 3H), 0.88–1.10 (m, 3H), 0.87 (s, 3H); ^{13}C NMR (100 MHz, $CDCl_3$): δ 183.4, 170.6, 57.2, 56.3, 54.9, 43.9, 43.6, 40.9, 40.7, 39.9, 39.5, 38.2, 37.9, 37.1, 29.1, 22.1, 21.6, 20.4, 19.0, 13.4; HRMS (ESI, *m/z*) calculated for $C_{20}H_{30}NO_3$ $[M-H]^-$: 332.2226; found: 332.2222.

Ethyl (4R,4aS,6aR,9S,11aR,11bS,E)-8-(hydroxyimino)-4,9,11b-trimethyltetradecahydro-6a,9-methanocyclohepta[a]naphthalene-4-carboxylate (6). To a solution of compound **2** (34.6 g, 0.1 mol) in EtOH (200 mL) was added $NH_2OH{\cdot}HCl$ (10.4 g, 0.15 mol) and $NaHCO_3$ (12.6 g, 0.15 mol). The mixture was stirred at 60 °C for 2 h. Then, the mixture was concentrated under vacuum, and the residue was extracted with CH_2Cl_2 and H_2O. The organic layer was washed with saturated aqueous NaCl, dried with $MgSO_4$ and concentrated under vacuum to give a white powder. Recrystallization of the powder from CH_2Cl_2–MeOH(1:1) afforded **6** as colorless crystals (33.2 g, 96%), m.p. 119.2–120.8 °C; X-ray crystal data can be obtained from the Cambridge Crystallographic Data Centre: CCDC 1577014; IR (KBr): 3305, 2943, 2847, 1722, 1450, 1233, 1179, 1152, 1028 cm^{-1}; ^1H NMR (400 MHz, $CDCl_3$): δ 4.11 (m, 2H), 2.99 (dd, $J = 3.1$, 18.6 Hz, 1H), 2.19 (d, $J = 13.4$ Hz, 1H), 2.00 (d, $J = 18.7$ Hz, 1H), 1.58–1.93 (m, 7H), 1.39–1.52 (m, 4H), 1.28 (t, $J = 7.2$ Hz, 3H), 1.21–1.26 (m, 2H), 1.20 (s, 3H), 1.13 (s, 3H), 0.84–1.12 (m, 4H), 0.79 (s, 3H); ^{13}C NMR (100 MHz, $CDCl_3$): δ 177.4, 170.9, 60.0, 57.1, 56.3, 54.9, 43.8, 43.7, 40.9, 40.6, 40.0, 39.5, 38.1, 38.0, 36.8, 28.9, 22.1, 21.7, 20.4, 18.9, 14.1, 13.4; HRMS (ESI, *m/z*) calculated for $C_{22}H_{36}NO_3$ $[M+H]^+$: 362.2695; found: 362.2685.

General Procedure for the Synthesis of Compounds 6a-r. To a cooled solution of compound 6 (361.0 mg, 1 mmol) in DMF (10 mL) was carefully added NaH (60% in oil, 48.0 mg, 1.2 mmol). The mixture was stirred at 0 °C for 1 h. A solution of R^1X (X = Cl, Br; 1.2 mmol) in DMF (5 mL) was then added dropwise to the mixture. The mixture was heated to 40 °C and stirred for 8–16 h. The reaction mixture was cooled and quenched at 0 °C with a saturated aqueous NH_4Cl. Then, the mixture was concentrated under vacuum to remove most of the DMF, and the residue was dissolved in CH_2Cl_2. After filtering, the filtrate was washed with saturated aqueous NaCl, dried with $MgSO_4$ and concentrated under vacuum. The crude material was purified by column chromatography (PE/EA) on silica gel to afford compounds **6a-r**. Detailed structural information is presented in the Supporting Information.

Ethyl (4R,4aS,6aR,9S,11aR,11bS,E)-8-(((2,5-dichlorobenzyl)oxy)imino)-4,9,11b-trimethyltetradecahydro-6a,9-methanocyclohepta[a]naphthalene-4-carboxylate (6a). Colorless crystal (yield 76%), m.p. 116.5–117.7 °C; X-ray crystal data can be obtained from the Cambridge Crystallographic Data Centre: CCDC 1554565; IR (KBr): 3077, 2926, 2847, 1716, 1645, 1463, 1377, 1236, 1039, 879 cm^{-1}; ^1H NMR (400 MHz, $CDCl_3$): δ 7.37 (d, $J = 2.4$ Hz, 1H), 7.25–7.29 (m, 1H), 7.16–7.21 (m, 1H), 5.16 (q, $J = 14.5$ Hz, 2H), 4.12 (m, 2H), 3.03 (dd, $J = 3.2$, 18.6 Hz, 1H), 2.19 (d, $J = 13.3$ Hz, 1H), 2.01 (d, $J = 18.6$ Hz, 1H), 1.56–1.93 (m, 7H), 1.37–1.51 (m, 4H), 1.29 (t, $J = 7.1$ Hz, 3H), 1.20–1.26 (m, 2H), 1.19 (s,

3H), 1.11–1.12 (m, 1H), 1.10 (s, 3H), 0.85–1.09 (m, 3H), 0.80 (s, 3H); ^{13}C NMR (100 MHz, $CDCl_3$): δ 177.4, 171.1, 138.5, 132.5, 130.7, 130.2, 128.7, 128.2, 71.9, 60.0, 57.2, 56.4, 54.9, 43.9, 43.7, 40.9, 40.8, 40.0, 39.7, 38.1, 38.0, 37.9, 28.9, 22.2, 21.7, 20.4, 19.0, 14.2, 13.4; HRMS (ESI, *m/z*) calculated for $C_{29}H_{40}Cl_2NO_3$ $[M+H]^+$: 520.2385; found: 520.2385.

Ethyl (4R,4aS,6aR,9S,11aR,11bS,E)-8-(((4-fluorobenzyl)oxy) imino)-4,9,11b-trimethyltetradecahydro-6a,9-methanocyclohe pta[a]naphthalene-4-carboxylate (6b). Colorless oil (yield 74%); IR (KBr): 3041, 2921, 2870, 2848, 1720, 1603, 1467, 1376, 1223, 1041, 834 cm^{-1}; ^{1}H NMR (400 MHz, $CDCl_3$): δ 7.36–7.29 (m, 2H), 7.01 (t, *J* = 8.6 Hz, 2H), 5.03 (s, 2H), 4.19–4.0 (m, 2H), 2.91 (dd, *J* = 18.6, 2.9 Hz 1H), 2.18 (d, *J* = 13.2 Hz 1H), 1.92 (d, *J* = 18.6 Hz 1H), 1.88–1.51 (m, 7H), 1.3–1.47 (m, 4H), 1.26 (t, *J* = 7.1 Hz 3H), 1.23–1.18 (m, 1H), 1.18 (s, 3H), 1.16–1.10 (m, 1H), 1.09 (s, 3H), 1.08–0.82 (m, 4H), 0.74 (s, 3H); ^{13}C NMR (100 MHz, $CDCl_3$): δ 177.3, 170.1, 162.3 (d, *J* = 243.9 Hz), 134.4 (d, *J* = 3.1 Hz), 129.7 (d, *J* = 7.9 Hz, 2C), 115.0 (d, *J* = 21.2 Hz, 2C), 74.6, 59.9, 57.2, 56.4, 54.9, 43.8, 43.7, 40.9, 40.7, 40.0, 39.6, 38.0, 37.9, 37.7, 28.9, 22.3, 21.7, 20.4, 19.0, 14.1, 13.4; ^{19}F NMR (376.3 MHz, $CDCl_3$): δ −114.9; HRMS (ESI, *m/z*) calculated for $C_{29}H_{41}FNO_3$ $[M+H]^+$: 470.3070; found: 470.3072.

Ethyl (4R,4aS,6aR,9S,11aR,11bS,E)-8-(((3-chlorobenzyl)oxy) imino)-4,9,11b-trimethyltetradecahydro-6a,9-methanocyclohe pta[a]naphthalene-4-carboxylate (6c). Colorless oil (yield 71%); IR (KBr): 3020, 2931, 2847, 1711, 1600, 1467, 1354, 1237, 1152, 777, 682 cm^{-1}; ^{1}H NMR (400 MHz, $CDCl_3$): δ 7.35 (s, 1H), 7.20–7.30 (m, 3H), 5.06 (s, 2H), 4.11 (m, 2H), 2.94 (dd, *J* = 3.0, 18.6 Hz, 1H), 2.18 (d, *J* = 13.2 Hz, 1H), 1.95 (d, *J* = 18.6 Hz, 1H), 1.55–1.91 (m, 8H), 1.36–1.48 (m,4H), 1.28 (t, *J* = 7.2 Hz, 3H), 1.20–1.24 (m, 1H), 1.19 (s, 3H), 1.10 (s, 3H), 0.83–1.09 (m, 4H), 0.76 (s, 3H); ^{13}C NMR (100 MHz, $CDCl_3$): δ 177.4, 170.6, 140.9, 134.1, 129.5, 127.9, 127.5, 125.8, 74.5, 60.0, 57.2, 56.4, 54.9, 43.9, 43.7, 40.9, 40.7, 40.0, 39.6, 38.1, 38.0, 37.8, 28.9, 22.3, 21.7, 20.4, 19.0, 14.2, 13.4; HRMS (ESI, *m/z*) calculated for $C_{29}H_{41}ClNO_3$ $[M+H]^+$: 486.2775; found: 486.2776.

Ethyl (4R,4aS,6aR,9S,11aR,11bS,E)-8-(((4-chloro-3-fluoroben zyl)oxy)imino)-4,9,11b-trimethyltetradecahydro-6a,9-methano cyclohepta[a]naphthalene-4-carboxylate (6d). White powder (yield 68%); IR (KBr): 3020, 2935, 2848, 1720, 1582, 1451, 1363, 1232, 1041, 872 cm^{-1}; ^{1}H NMR (400 MHz, $CDCl_3$): δ 7.36 (t, *J* = 8.2 Hz, 1H), 7.15 (d, *J* = 8.2 Hz, 1H), 7.06 (d, *J* = 8.2 Hz, 1H), 5.03 (s, 2H), 4.11 (m, 2H), 2.94 (d, *J* = 18.5 Hz, 1H), 2.19 (d, *J* = 13.2 Hz, 1H), 1.94 (d, *J* = 18.7 Hz, 1H), 1.54–1.90 (m, 8H), 1.36–1.49 (m, 4H), 1.28 (t, *J* = 7.0 Hz, 3H), 1.21–1.25 (m, 1H), 1.19 (s, 3H), 1.10–1.12 (m, 1H), 1.09 (s, 3H), 0.83–1.06 (m, 3H), 0.76 (s, 3H); ^{13}C NMR (100 MHz, $CDCl_3$): δ 177.3, 170.7, 158.0 (d, *J* = 247.1 Hz), 139.9 (d, *J* = 6.3 Hz), 130.3, 123.9 (d, *J* = 3.4 Hz), 119.7 (d, *J* = 17.5 Hz), 115.8 (d, *J* = 21.1 Hz), 73.9, 60.0, 57.2, 56.4, 54.9, 43.9, 43.7, 40.9, 40.7, 40.0, 39.6, 38.1, 38.0, 37.8, 29.0, 22.2, 21.7, 20.4, 19.0, 14.1, 13.4; ^{19}F NMR (376.3 MHz, $CDCl_3$): δ −115.8; HRMS (ESI, *m/z*) calculated for $C_{29}H_{40}ClFNO_3$ $[M+H]^+$: 504.2681; found: 504.2680.

Ethyl (4R,4aS,6aR,9S,11aR,11bS,E)-4,9,11b-trimethyl-8-(((4-(trifluoromethyl)benzyl)oxy)imino)tetradecahydro-6a,9-methanocyclohepta[a]naphthalene-4-carboxylate (6e). White powder (yield 73%); IR (KBr): 3020, 2937, 2848, 1720, 1620, 1453, 1326, 1232, 1066, 843 cm^{-1}; ^{1}H NMR (400 MHz, $CDCl_3$): δ 7.61 (d, *J* = 7.1 Hz, 2H), 7.46 (d, *J* = 7.1 Hz, 2H), 5.14 (s, 2H), 4.11 (m, 2H), 2.96 (d, *J* = 18.7 Hz, 1H), 2.19 (d, *J* = 13.4 Hz, 1H), 1.96 (d, *J* = 18.5 Hz, 1H), 1.48–1.92 (m, 8H), 1.37–1.48 (m, 4H), 1.28 (t, *J* = 6.4 Hz, 3H), 1.21–1.24 (m, 1H), 1.19 (s, 3H), 1.11–1.17 (m, 1H), 1.10 (s, 3H), 0.81–1.08 (m, 3H), 0.76 (s, 3H); ^{13}C NMR (100 MHz, $CDCl_3$): δ 177.3, 170.6, 142.9, 129.6 (q, *J* = 32.0 Hz), 127.8 (2C), 125.1 (q, *J* = 3.6Hz, 2C), 124.2 (q, *J* = 270.4 Hz), 74.5, 60.0, 57.2, 56.4, 54.9, 43.9, 43.7, 40.9, 40.7, 40.0, 39.6, 38.1, 38.0, 37.8, 28.9, 22.2, 21.7, 20.4, 19.0, 14.1, 13.4; ^{19}F NMR (376.3 MHz, $CDCl_3$) δ −62.5; HRMS (ESI, *m/z*) calculated for $C_{30}H_{41}F_3NO_3$ $[M+H]^+$: 520.3039; found: 520.3037.

Ethyl (4R,4aS,6aR,9S,11aR,11bS,E)-4,9,11b-trimethyl-8-(((4-(trifluoromethoxy)benzyl)oxy)imino)tetradecahydro-6a,9-methanocyclohepta[a]naphthalene-4-carboxylate (6f). White powder (yield 72%); IR (KBr): 3020, 2937, 2848, 1720, 1608, 1453, 1260, 1018, 844 cm^{-1}; ^{1}H NMR (400 MHz, $CDCl_3$): δ 7.39 (d, *J* = 7.8 Hz, 2H), 7.19 (d, *J* = 7.8 Hz, 2H), 5.08 (s, 2H), 4.11 (m, 2H), 2.93 (d, *J* = 18.6 Hz, 1H), 2.19 (d, *J* = 13.4 Hz, 1H), 1.94 (d, *J* = 18.6 Hz, 1H), 1.54–1.90 (m, 8H), 1.36–1.48 (m, 4H), 1.28 (t, *J* = 7.2 Hz, 3H), 1.20–1.23 (m, 1H), 1.19 (s, 3H), 1.11–1.17 (m, 1H), 1.10 (s, 3H), 0.83–1.07 (m, 3H), 0.74 (s, 3H); ^{13}C NMR (100 MHz, $CDCl_3$): δ 177.3, 170.5, 148.6, 137.5, 129.3 (2C), 120.7 (2C), 120.5 (d, *J* = 255.2 Hz), 74.4, 60.0, 57.2, 56.4, 54.9, 43.8, 43.7, 40.9, 40.7, 40.0, 39.6, 38.0, 38.0, 37.8, 28.9, 22.2, 21.7, 20.4, 19.0, 14.1, 13.4; ^{19}F NMR (376.3 MHz, $CDCl_3$): δ −57.8; HRMS (ESI, *m/z*) calculated for $C_{30}H_{41}F_3NO_4$ $[M+H]^+$: 536.2988; found: 536.2980.

Ethyl (4R,4aS,6aR,9S,11aR,11bS,E)-4,9,11b-trimethyl-8-(((per-fluorophenyl)methoxy) imino)tetradecahydro-6a,9-methanocyclohepta[a]naphthalene-4-carboxylate (6g). White powder (yield 68%); IR (KBr): 3020, 2957, 2928, 2850, 1721, 1655, 1507, 1455, 1365, 1218, 1027, 868 cm^{-1}; ^{1}H NMR (400 MHz, $CDCl_3$): δ 5.10 (s, 2H), 4.08 (m, 2H), 2.83 (dd, *J* = 3.0, 18.6 Hz, 1H), 2.15 (d, *J* = 13.2 Hz, 1H), 1.49–1.87 (m, 8H), 1.32–1.43 (m, 4H), 1.25 (t, *J* = 7.1 Hz, 3H), 1.16–1.20 (m, 1H), 1.15 (s, 3H), 1.03–1.14 (m, 2H), 1.02 (s, 3H), 0.78–1.00 (m, 3H), 0.71 (s, 3H); ^{13}C NMR (100 MHz, $CDCl_3$): δ 177.2, 171.0, 159.7, 145.7 (m, 2C), 137.3 (m, 2C), 111.8, 61.9, 59.9, 57.1, 56.2, 54.9, 43.8, 43.6, 40.8, 40.7, 39.9, 39.6, 38.0 (2C), 37.3, 28.8, 21.9, 21.6, 20.3, 18.9, 14.0, 13.2; ^{19}F NMR (376.3 MHz, $CDCl_3$): δ −142.1, −154.4, −162.7; HRMS (ESI, *m/z*) calculated for $C_{29}H_{37}F_5NO_3$ $[M+H]^+$: 542.2694; found: 542.2686.

Ethyl 5-(((((4R,4aS,6aR,9S,11aR,11bS,E)-4-(ethoxycarbonyl)-4,9,11b-trimethyldodecahydro-6a,9-methanocyclohepta[a] naphthalen-8(7H)-ylidene)amino)oxy)methyl)furan-2-carboxylate (6h). Colourless crystal (318.7 mg, 62%), m.p. 66.1–66.8 °C; X-ray crystal file is available from the Cambridge Crystallographic Data Centre: CCDC 1577015; IR (KBr): 3020, 2937, 2848, 1720, 1595, 1453, 1365, 1210, 1022 cm^{-1}; ^{1}H NMR (400 MHz, $CDCl_3$): δ 7.05 (d, *J* = 3.4 Hz, 1H), 6.35 (d, *J* = 3.4 Hz, 1H), 4.96 (s, 2H), 4.28 (q, *J* = 7.1 Hz, 2H), 4.02 (m, 2H), 2.81 (dd, *J* = 3.0, 18.6 Hz, 1H), 2.09 (d, *J* = 13.2 Hz, 1H), 1.83 (d, *J* = 18.7 Hz, 1H), 1.45–1.79 (m, 7H), 1.32–1.38 (m, 4H), 1.30 (t, *J* = 7.1 Hz, 3H), 1.20 (t, *J* = 7.2 Hz, 3H), 1.11–1.14 (m, 1H), 1.10 (s, 3H), 1.03–1.09 (m, 1H), 1.01 (s, 3H), 0.74–0.99 (m, 4H), 0.65 (s, 3H); ^{13}C NMR (100 MHz, $CDCl_3$): δ 177.2, 170.6, 158.6, 156.5, 144.2, 118.5, 110.7, 67.2, 60.7, 59.9, 57.1, 56.3, 54.8, 43.8, 43.6, 40.8, 40.6, 39.9, 39.5, 38.0 (2C), 37.5, 28.8, 22.2, 21.6, 20.3, 18.9, 14.3, 14.1, 13.3; HRMS (ESI, *m/z*) calculated for $C_{30}H_{44}NO_6$ $[M+H]^+$: 514.3169; found: 514.3171.

Ethyl (4R,4aS,6aR,9S,11aR,11bS,E)-8-(((5-chlorobenzo[b]thiophen-3-yl)methoxy)imino)-4,9,11b-trimethyltetradecahydro-6a,9-methanocyclohepta[a]naphthalene-4-carboxylate (6i). Yellow powder (396.2 mg, 73%); IR (KBr): 3093, 2927, 2848, 1717, 1587, 1452, 1361, 1219, 1028, 834 cm^{-1}; ^{1}H NMR (400 MHz, $CDCl_3$): δ 7.95 (d, *J* = 1.9 Hz, 1H), 7.75 (d, *J* = 8.6 Hz, 1H), 7.4 (s, 1H), 7.31 (dd, *J* = 1.9, 8.6 Hz, 1H), 5.26 (s, 2H), 4.09 (m, 2H), 2.88 (dd, *J* = 3.1, 18.6 Hz, 1H), 2.17 (d, *J* = 13.2 Hz, 1H), 1.89 (d, *J* = 18.6 Hz, 1H), 1.52–1.85 (m, 7H), 1.34–1.45 (m, 4H), 1.26 (t, *J* = 7.1 Hz, 3H), 1.17 (s, 3H), 1.13 (s, 3H), 0.78–1.12 (m, 6H), 0.64 (s, 3H); ^{13}C NMR (100 MHz, $CDCl_3$): δ 177.3, 170.5, 139.7, 138.6, 133.4, 130.5, 127.1, 124.8, 123.6, 122.5, 69.4, 60.0, 57.1, 56.4, 54.9, 43.9, 43.7, 40.9, 40.7, 39.9, 39.7, 38.0, 38.0, 37.6, 28.9, 22.3, 21.7, 20.3, 19.0, 14.2, 13.2; HRMS (ESI, *m/z*) calculated for $C_{31}H_{41}ClNO_3S$ $[M+H]^+$: 542.2496; found: 542.2495.

Ethyl (4R,4aS,6aR,9S,11aR,11bS,E)-8-(((2-chlorothiazol-5-yl) methoxy)imino)-4,9,11b-trimethyltetradecahydro-6a,9-methanocyclohepta[a]naphthalene-4-carboxylate (6j). Yellow oil (320.9 mg, 65%); IR (KBr): 3020, 2927, 2848, 1720, 1530, 1454, 1377, 1232, 1047, 869 cm^{-1}; ^{1}H NMR (400 MHz, $CDCl_3$): δ 7.4 (s, 1H),

5.1 (s, 2H), 4.1 (m, 2H), 2.87 (dd, $J = 2.7$, 18.6 Hz, 1H), 2.18 (d, $J = 13.1$ Hz, 1H), 1.58−1.91 (m, 8H), 1.38−1.48 (m, 4H), 1.27 (t, $J = 7.1$ Hz, 3H), 1.20−1.24 (m, 2H), 1.18 (s, 3H), 1.13 (s, 3H), 0.82−1.08 (m, 4H), 0.74 (s, 3H); ^{13}C NMR (100 MHz, $CDCl_3$): δ 177.3, 171.3, 152.6, 139.5, 137.9, 67.2, 60.0, 57.1, 56.3, 54.9, 44.1, 43.7, 40.8, 40.8, 39.9, 39.6, 38.0, 38.0, 37.6, 28.9, 22.2, 21.6, 20.4, 19.0, 14.1, 13.4; HRMS (ESI, m/z) calculated for $C_{26}H_{38}ClN_2O_3S$ $[M+H]^+$: 493.2292; found: 493.2289.

Ethyl (4R,4aS,6aR,9S,11aR,11bS,E)-4,9,11b-trimethyl-8-((thiophen-3-ylmethoxy)imino)tetradecahydro-6a,9-methanocyclohepta[a]naphthalene-4-carboxylate (6k). Pale yellow powder (yield 78%); IR (KBr): 3103, 2936, 2847, 1720, 1656, 1452, 1376, 1232, 1028 cm^{-1}; ^{1}H NMR (400 MHz, $CDCl_3$): δ 7.25−7.28 (m, 1H), 7.21−7.24 (m, 1H), 7.09−7.13 (m, 1H), 5.08 (s, 2H), 4.10 (m, 2H), 2.91 (dd, $J = 3.1$, 18.6 Hz, 1H), 2.18 (d, $J = 13.3$ Hz, 1H), 1.92 (d, $J = 18.6$ Hz, 1H), 1.54−1.88 (m, 7H), 1.36−1.47 (m, 4H), 1.27 (t, $J = 7.1$ Hz, 3H), 1.19−1.24 (m, 1H), 1.18 (s, 3H), 1.13−1.17 (m, 1H), 1.12 (s, 3H), 0.83−1.08 (m, 4H), 0.74 (s, 3H); ^{13}C NMR (100 MHz, $CDCl_3$): δ 177.3, 169.9, 139.7, 127.7, 125.5, 123.0, 70.6, 59.9, 57.2, 56.4, 55.0, 43.8, 43.7, 40.9, 40.7, 40.0, 39.6, 38.0 (2C), 37.7, 29.0, 22.3, 21.7, 20.4, 19.0, 14.2, 13.4; HRMS (ESI, m/z) calculated for $C_{27}H_{40}NO_3S$ $[M+H]^+$: 458.2729; found: 458.2715.

Ethyl (4R,4aS,6aR,9S,11aR,11bS,E)-8-(((1,3-dimethyl-1H-pyrazol-5-yl)methoxy)imino)-4,9,11b-trimethyltetradecahydro-6a,9-methanocyclohepta[a]naphthalene-4-carboxylate (6l). Colourless oil (347.2 mg, 74%); IR (KBr): 3020, 2937, 2848, 1720, 1655, 1455, 1376, 1232, 1051 cm^{-1}; ^{1}H NMR (400 MHz, $CDCl_3$): δ 6.02 (s, 1H), 4.96 (s, 2H), 4.08 (m, 2H), 3.82 (s, 3H), 2.84 (dd, $J = 3.1$, 18.6 Hz, 1H), 2.23 (s, 3H), 2.15 (d, $J = 13.3$ Hz, 1H), 1.51−1.88 (m, 8H), 1.34−1.44 (m, 4H), 1.25 (t, $J = 7.2$ Hz, 3H), 1.17−1.21 (m, 1H), 1.16 (s, 3H), 1.08−1.14 (m, 1H), 1.07 (s, 3H), 0.79−1.04 (m, 4H), 0.70 (s, 3H); ^{13}C NMR (100 MHz, $CDCl_3$): δ 177.3, 170.5, 147.0, 139.7, 106.5, 65.3, 60.0, 57.1, 56.3, 54.9, 43.8, 43.7, 40.8, 40.7, 39.9, 39.6, 38.0, 38.0, 37.5, 36.4, 28.9, 22.2, 21.6, 20.3, 18.9, 14.2, 13.4, 13.3; HRMS (ESI, m/z) calculated for $C_{28}H_{44}N_3O_3$ $[M+H]^+$: 470.3383; found: 470.3373.

Ethyl (4R,4aS,6aR,9S,11aR,11bS,E)-8-(((3,5-dimethylisoxazol-4-yl)methoxy)imino)-4,9,11b-trimethyltetradecahydro-6a,9-methanocyclohepta[a]naphthalene-4-carboxylate (6m). White powder (334.9 mg, 71%); IR (KBr): 3020, 2933, 2847, 1719, 1637, 1452, 1376, 1231, 1015 cm^{-1}; ^{1}H NMR (400 MHz, $CDCl_3$): δ 4.66 (s, 2H), 3.97 (m, 2H), 2.71 (dd, $J = 2.6$, 18.5 Hz, 1H), 2.27 (s, 3H), 2.15 (s, 3H), 2.04 (d, $J = 13.1$ Hz, 1H), 1.39−1.77 (m, 8H), 1.23−1.34 (m, 4H), 1.14 (t, $J = 7.1$ Hz, 3H), 1.06−1.12 (m, 1H), 1.05 (s, 3H), 0.96−1.03 (m, 2H), 0.94 (s, 3H), 0.69−0.92 (m, 3H), 0.60 (s, 3H); ^{13}C NMR (100 MHz, $CDCl_3$): δ 177.0, 169.9, 167.5, 159.8, 111.5, 63.7, 59.8, 57.0, 56.1, 54.7, 43.6, 43.5, 40.7, 40.5, 39.8, 39.6, 37.9, 37.9, 37.3, 28.8, 22.1, 21.5, 20.2, 18.9, 14.1, 13.2, 11.0, 10.0; HRMS (ESI, m/z) calculated for $C_{28}H_{43}N_2O_4$ $[M+H]^+$: 471.3223; found: 471.3224.

Ethyl (4R,4aS,6aR,9S,11aR,11bS,E)-4,9,11b-trimethyl-8-(((tetrahydro-2H-pyran-4-yl)oxy)imino)tetradecahydro-6a,9-methanocyclohepta[a]naphthalene-4-carboxylate (6n). Colourless oil (308.6 mg, 69%); IR (KBr): 2953, 2928, 2848, 1722, 1452, 1381, 1260, 1067 cm^{-1}; ^{1}H NMR (400 MHz, $CDCl_3$): δ 4.25 (m, 1H), 4.11 (m, 2H), 3.91 (m, 2H), 3.52 (m, 2H), 2.93 (dd, $J = 3.2$, 18.6 Hz, 1H), 2.18 (d, $J = 13.2$ Hz, 1H), 1.56−1.96 (m, 12H), 1.37−1.46 (m, 4H), 1.28 (t, $J = 7.1$ Hz, 3H), 1.19−1.25 (m, 2H), 1.18 (s, 3H), 1.09 (s, 3H), 0.84−1.07 (m, 4H), 0.76 (s, 3H); ^{13}C NMR (100 MHz, $CDCl_3$): δ 177.3, 169.9, 76.0, 65.6 (2C), 60.0, 57.2, 56.5, 55.0, 43.7 (2C), 41.0, 40.7, 40.0, 39.7, 38.1, 38.0, 37.6, 32.1, 29.7, 29.0, 22.3, 21.7, 20.5, 19.0, 14.1, 13.4; HRMS (ESI, m/z) calculated for $C_{27}H_{44}NO_4$ $[M+H]^+$: 446.3270; found: 446.3282.

Ethyl (4R,4aS,6aR,9S,11aR,11bS,E)-8-(((1,3-dioxolan-2-yl)methoxy)imino)-4,9,11b-trimethyltetradecahydro-6a,9-methanocyclohepta[a]naphthalene-4-carboxylate (6o). Colourless oil (327.4 mg, 73%); IR (KBr): 2958, 2847, 1720, 1454, 1377, 1233, 1050 cm^{-1}; ^{1}H NMR (400 MHz, $CDCl_3$): δ 5.16 (t, $J = 4.2$ Hz, 1H), 4.00−4.18 (m, 4H), 3.86−4.00 (m, 4H), 2.91 (dd, $J = 2.9$, 18.6 Hz, 1H), 2.15 (d, $J = 13.2$ Hz, 1H), 1.95 (d, $J = 18.7$ Hz, 1H), 1.53−1.86 (m, 7H), 1.34−1.46 (m, 4H), 1.26 (t, $J = 7.2$ Hz, 3H), 1.17−1.23 (m, 2H), 1.16 (s, 3H), 1.07 (s, 3H), 0.80−1.05 (m, 4H), 0.74 (s, 3H); ^{13}C NMR (100 MHz, $CDCl_3$): δ 177.4, 170.1, 102.1, 74.1, 65.1, 65.0, 60.0, 57.1, 56.4, 55.0, 43.8, 43.7, 40.9, 40.6, 40.0, 39.5, 38.0 (2C), 37.4, 28.9, 22.2, 21.7, 20.4, 18.9, 14.2, 13.3; HRMS (ESI, m/z) calculated for $C_{26}H_{42}NO_5$ $[M+H]^+$: 448.3063; found: 448.3055.

Ethyl (4R,4aS,6aR,9S,11aR,11bS,E)-4,9,11b-trimethyl-8-(((3-methyloxetan-3-yl)methoxy)imino)tetradecahydro-6a,9-methanocyclohepta[a]naphthalene-4-carboxylate (6p). White powder (yield 76%); IR (KBr): 2930.9, 2849.1, 1721.9, 1452.7, 1379.1, 1231.7, 1152.3, 1042.7 cm^{-1}; ^{1}H NMR (400 MHz, $CDCl_3$): δ 4.65−4.61 (m, 2H), 4.33−4.30 (m, 2H), 4.18−4.01 (m, 4H), 2.9 (dd, $J = 18.6$, 3.1 Hz, 1H), 2.17 (d, $J = 13.2$ Hz, 1H), 1.89 (d, $J = 18.5$ Hz, 1H), 1.86−1.53 (m, 7H), 1.47−1.35 (m, 4H), 1.33 (s, 3H), 1.26 (t, $J = 7.1$, 3H), 1.24−1.18 (m, 2H), 1.17 (s, 3H), 1.07 (s, 3H), 1.06−0.81 (m, 4H), 0.75 (s, 3H); ^{13}C NMR (100 MHz, $CDCl_3$): δ 177.3, 169.6, 80.3, 80.2, 77.7, 59.9, 57.2, 56.3, 54.9, 43.7, 43.6, 40.9, 40.7, 40.3, 39.9, 39.6, 38.1, 38.0, 37.3, 29.0, 22.2, 21.6, 21.5, 20.4, 19.0, 14.1, 13.3; HRMS (ESI, m/z) calculated for $C_{27}H_{44}NO_4$ $[M+H]^+$: 446.3270; found: 446.3274.

Ethyl (4R,4aS,6aR,9S,11aR,11bS,E)-4,9,11b-trimethyl-8-((2-morpholinoethoxy)imino)tetradecahydro-6a,9-methanocyclohepta[a]naphthalene-4-carboxylate (6q). Colourless oil (314.5 mg, 66%); IR (KBr): 2954, 2847, 1720, 1450, 1363, 1231, 1034 cm^{-1}; ^{1}H NMR (400 MHz, $CDCl_3$): δ 4.12 (t, $J = 5.7$ Hz, 2H), 4.04 (m, 2H), 3.64 (t, $J = 4.6$ Hz, 4H), 2.82 (dd, $J = 2.9$, 18.5 Hz, 1H), 2.59 (m, 2H), 2.41−2.52 (m, 4H), 2.11 (d, $J = 13.2$ Hz, 1H), 1.82 (d, $J = 18.5$ Hz, 1H), 1.47−1.80 (m, 7H), 1.30−1.41 (m, 4H), 1.21 (t, $J = 7.2$ Hz, 3H), 1.13−1.18 (m, 2H), 1.11 (s, 3H), 1.03 (s, 3H), 0.77−1.01 (m, 4H), 0.68 (s, 3H); ^{13}C NMR (100 MHz, $CDCl_3$): δ 177.2, 169.3, 71.3, 66.9 (2C), 59.9, 57.6, 57.1, 56.4, 54.9, 54.1 (2C), 43.6, 43.6, 40.9, 40.6, 39.9, 39.6, 38.0, 37.9, 37.6, 28.9, 22.3, 21.6, 20.4, 18.9, 14.1, 13.3; HRMS (ESI, m/z) calculated for $C_{28}H_{47}N_2O_4$ $[M+H]^+$: 475.3536; found: 475.3528.

Ethyl (4R,4aS,6aR,9S,11aR,11bS,E)-8-((allyloxy)imino)-4,9,11b-trimethyltetradecahydro-6a,9-methanocyclohepta[a]naphthalene-4-carboxylate (6r). Colourless oil (310.2 mg, 77%); IR (KBr): 3078.9, 2937.4, 2847.7, 1720.7, 1655.4, 1453.5, 1418.6, 1376.5, 1231.9, 1178.7, 1030.7, 921.7 cm^{-1}; ^{1}H NMR (400 MHz, $CDCl_3$): δ 6.07 (m, 1H), 5.27 (d, $J = 17.3$ Hz, 1H), 5.18 (d, $J = 10.4$ Hz, 1H), 4.54 (d, $J = 5.1$ Hz, 2H), 4.2−4.0 (m, 2H), 2.97−2.88 (m, 1H), 2.18 (d, $J = 13.2$, 1H), 1.94 (d, $J = 18.6$, 1H), 1.90−1.53 (m, 8H), 1.48−1.36 (m, 4H), 1.27 (t, $J = 7.1$ Hz, 3H), 1.24−1.19 (m, 1H), 1.18, (s, 3H), 1.10 (s, 3H), 1.09−0.83 (m, 4H), 0.77 (s, 3H); ^{13}C NMR (100 MHz, $CDCl_3$): δ 177.4, 169.6, 134.8, 116.7, 74.3, 59.9, 57.2, 56.5, 55.0, 43.7, 43.7, 40.9, 40.6, 40.0, 39.6, 38.1, 38.0, 37.5, 29.0, 22.2, 21.7, 20.5, 19.0, 14.1, 13.4; HRMS (ESI, m/z) calculated for $C_{25}H_{40}NO_3$ $[M+H]^+$: 402.3008; found: 402.2998.

General Procedure for the Synthesis of Compounds 6ra-rq. To a solution of compound 6r (401.3 mg, 1 mmol), $Pd(OAc)_2$ (22.5 mg, 0.1 mmol), P(O-Tolyl)$_3$ (60.9 mg, 0.2 mmol), and Et_3N (303.6 mg, 417 μL, 3 mmol) in ACN (10 mL) under an argon atmosphere in a sealed tube was added a solution of R^2X (heteroaryl or aryl halides, X = Br, I; 1.5 mmol) in ACN (5 mL) dropwise. The mixture was stirred under an argon atmosphere at 40 °C for 16−48 h. The reaction mixture was then cooled and concentrated under vacuum, and the residue was dissolved in CH_2Cl_2. After filtration, the filtrate was washed with saturated aqueous NaCl, dried with $MgSO_4$ and concentrated under vacuum. The crude material was purified by column chromatography (PE/EA) on silica gel to afford compounds **6ra-rq**. Detailed structural information is described in the Supporting Information.

Ethyl (4R,4aS,6aR,9S,11aR,11bS,E)-8-((cinnamyloxy)imino)-

4,9,11b-trimethyltetradecahydro-6a,9-methanocyclohepta[a] naphthalene-4-carboxylate (6ra). Colourless crystal (391.8 mg, 82%), m.p. 104.0−104.5 °C; X-ray crystal file is available from the Cambridge Crystallographic Data Centre: CCDC 1577016; IR (KBr): 3025, 2926, 2847, 1721, 1599, 1451, 1365, 1232, 1029 cm^{-1}; ^1H NMR (400 MHz, $CDCl_3$): δ 7.40−7.44 (m, 2H), 7.31−7.36 (m, 2H), 7.23−7.28 (m, 1H), 6.63 (d, J = 16.0, 1H), 6.39 (dt, J = 6.1, 16.0 Hz, 1H), 4.72 (d, J = 6.1 Hz, 2H), 4.11 (m, 2H), 2.96 (dd, J = 3.1, 18.6 Hz, 1H), 2.19 (d, J = 13.2 Hz, 1H), 1.98 (d, J = 18.6 Hz, 1H), 1.62−1.87 (m, 7H), 1.40−1.49 (m, 4H), 1.28 (t, J = 7.2 Hz, 3H), 1.21−1.25 (m, 1H), 1.19 (s, 3H), 1.13 (s, 3H), 0.84−1.09 (m, 5H), 0.79 (s, 3H); ^{13}C NMR (100 MHz, $CDCl_3$): δ 177.5, 169.8, 136.9, 132.4, 128.5 (2C), 127.6, 126.5 (2C), 126.1, 74.1, 60.0, 57.2, 56.5, 55.0, 43.8, 43.7, 41.0, 40.7, 40.0, 39.6, 38.1, 38.0, 37.6, 28.9, 22.3, 21.7, 20.5, 19.0, 14.2, 13.4; HRMS (ESI, m/z) calculated for $C_{31}H_{44}NO_3$ $[M+H]^+$: 478.3321; found: 478.3322.

Ethyl (4R,4aS,6aR,9S,11aR,11bS,E)-8-((((E)-3-(4-fluorophenyl) allyl)oxy)imino)-4,9,11b-trimethyltetradecahydro-6a,9-methanocyclohepta[a]naphthalene-4-carboxylate (6rb). White powder (416.5 mg, 84%); IR (KBr): 3020, 2928, 2848, 1721, 1601, 1509, 1453, 1372, 1231, 1027, 846 cm-1; 1H NMR (400 MHz, CDCl3): δ 7.31−7.37 (m, 2H), 6.95−7.02 (m, 2H), 6.56 (d, J = 16.0 Hz, 1H), 6.28 (dt, J = 6.1, 16.0 Hz, 1H), 4.68 (d, J = 6.1 Hz, 2H), 4.08 (m, 2H), 2.93 (dd, J = 3.0, 18.6 Hz, 1H), 2.17 (d, J = 13.2 Hz, 1H), 1.96 (d, J = 18.6 Hz, 1H), 1.55−1.87 (m,7H), 1.36−1.46 (m, 4H), 1.25 (t, J = 7.1 Hz, 3H), 1.18−1.23 (m, 1H), 1.17 (s, 3H), 1.11 (s, 3H), 0.81−1.09 (m, 5H), 0.76 (s, 3H); 13C NMR (100 MHz, CDCl3): δ 177.3, 169.6, 162.3 (d, J = 245.3 Hz), 133.1 (d, J = 3.2 Hz), 131.2, 128.0 (d, J = 7.9 Hz, 2C), 125.8 (d, J = 1.6 Hz), 115.4 (d, J = 21.4 Hz, 2C), 74.0, 59.9, 57.1, 56.5, 55.0, 43.8, 43.7, 40.9, 40.7, 40.0, 39.6, 38.0, 38.0, 37.6, 28.9, 22.3, 21.7, 20.5, 19.0, 14.2, 13.4; 19F NMR (376.3 MHz, CDCl3): δ −114.3; HRMS (ESI, m/z) calculated for $C_{31}H_{43}FNO_3$ $[M+H]^+$: 496.3227; found: 496.3224.

Ethyl (4R,4aS,6aR,9S,11aR,11bS,E)-4,9,11b-trimethyl-8-((((E)-3-(3-(trifluoromethyl)phenyl)allyl)oxy)imino)tetradecahydro-6a,9-methanocyclohepta[a]naphthalene-4-carboxylate (6rc). White powder (443.3 mg, 81%); IR (KBr): 3020, 2934, 2848, 1721, 1450, 1364, 1332, 1129, 879,698 cm^{-1}; ^1H NMR (400 MHz, $CDCl_3$): δ7.61 (s, 1H), 7.53 (d, J = 7.6 Hz, 1H), 7.46 (d, J = 7.6 Hz, 1H), 7.36−7.42 (m, 1H), 6.61 (d, J = 16.0 Hz, 1H), 6.43 (dt, J = 5.8, 16.0 Hz, 1H), 4.71 (d, J = 5.8 Hz, 2H), 4.08 (m, 2H), 2.96 (dd, J = 2.8, 18.5 Hz, 1H), 2.17 (d, J = 13.2 Hz, 1H), 1.97 (d, J = 18.6 Hz, 1H), 1.56−1.89 (m, 7H), 1.37−1.47 (m, 4H), 1.24 (t, J = 7.1 Hz, 3H), 1.18−1.21 (m, 1H), 1.17 (s, 3H), 1.11 (s, 3H), 0.81−1.09 (m, 5H), 0.77 (s, 3H); ^{13}C NMR (100 MHz, $CDCl_3$): δ177.3, 169.8, 137.7, 130.9 (q, J = 31.8 Hz), 130.6, 129.6, 128.9, 128.4, 124.1 (q, J = 270.6 Hz), 124.0 (q, J = 3.7 Hz), 123.1 (q, J = 3.8 Hz), 73.6, 59.9, 57.1, 56.4, 54.9, 43.8, 43.7, 40.9, 40.7, 39.9, 39.6, 38.0, 38.0, 37.6, 28.9, 22.3, 21.7, 20.5, 19.0, 14.1, 13.4; ^{19}F NMR (376.3 MHz, $CDCl_3$) δ −62.7; HRMS (ESI, m/z) calculated for $C_{32}H_{43}F_3NO_3$ $[M+H]^+$: 546.3195; found: 546.3199.

Ethyl (4R,4aS,6aR,9S,11aR,11bS,E)-4,9,11b-trimethyl-8-((((E)-3-(4-(trifluoromethoxy)phenyl)allyl)oxy)imino)tetradecahydro-6a,9-methanocyclohepta[a]naphthalene-4-carboxylate (6th**).** White powder (461.4 mg, 82%); IR (KBr): 3020, 2928, 2848, 1721, 1508, 1453, 1376, 1259, 1029 cm^{-1}; ^1H NMR (400 MHz, $CDCl_3$): δ 7.41 (d, J = 8.3 Hz, 2H), 7.17 (d, J = 8.3 Hz, 2H), 6.60 (d, J = 16.0 Hz, 1H), 6.36 (dt, J = 5.8, 16.0 Hz, 1H), 4.71 (d, J = 5.8 Hz, 2H), 4.11 (m, 2H), 2.96 (dd, J = 2.4, 18.5 Hz, 1H), 2.19 (d, J = 13.2 Hz, 1H), 1.97 (d, J = 18.6 Hz, 1H), 1.56−1.92 (m, 8H), 1.38−1.50 (m, 4H), 1.28 (t, J = 7.0 Hz, 3H), 1.21−1.25 (m, 1H), 1.19 (s, 3H), 1.12 (s, 3H), 0.85−1.10 (m, 4H), 0.78 (s, 3H); ^{13}C NMR (100 MHz, $CDCl_3$): δ177.3, 169.8, 148.5, 135.8, 130.7, 127.7 (2C), 127.4, 121.0 (2C), 120.5 (q, J = 255.5 Hz), 73.8, 59.9, 57.2, 56.5, 55.0, 43.8, 43.7, 41.0, 40.7, 40.0, 39.6, 38.1, 38.0, 37.6, 28.9, 22.3, 21.7, 20.5, 19.0, 14.1, 13.4; ^{19}F NMR (376.3 MHz, $CDCl_3$): δ −57.9; HRMS (ESI, m/z) calculated for $C_{32}H_{43}F_3NO_4$ $[M+H]^+$: 562.3144; found: 562.3146.

Ethyl (4R,4aS,6aR,9S,11aR,11bS,E)-8-((((E)-3-(4-cyanophenyl) allyl)oxy)imino)-4,9,11b-trimethyltetradecahydro-6a,9-methanocyclohepta[a]naphthalene-4-carboxylate (6re). Colourless oil (392.8 mg, 78%); IR (KBr): 3020, 2952, 2848, 1715, 1565, 1445, 1363, 1217, 1027 cm^{-1}; ^1H NMR (400 MHz, $CDCl_3$): δ 7.61 (d, J = 8.3 Hz, 2H), 7.48 (d, J = 8.3 Hz, 2H), 6.62 (d, J = 16.1 Hz, 1H), 6.50 (dt, J = 5.5, 16.1 Hz, 1H), 4.74 (d, J = 5.5 Hz, 2H), 4.10 (m, 2H), 2.95 (dd, J = 3.1, 18.6 Hz, 1H), 2.19 (d, J = 13.2 Hz, 1H), 1.97 (d, J = 18.6 Hz, 1H), 1.60−1.90 (m, 8H), 1.38−1.49 (m, 4H), 1.28 (t, J = 7.2 Hz, 3H), 1.21−1.25 (m, 1H), 1.19 (s, 3H), 1.12 (s, 3H), 0.83−1.09 (m, 4H), 0.78 (s, 3H); ^{13}C NMR (100 MHz, $CDCl_3$): δ 177.4, 170.1, 141.5, 132.4 (2C), 130.5, 130.2, 126.9 (2C), 119.0, 110.8, 73.5, 60.0, 57.2, 56.5, 54.9, 43.9, 43.7, 40.9, 40.7, 40.0, 39.6, 38.1, 38.0, 37.6, 29.0, 22.3, 21.7, 20.5, 19.0, 14.1, 13.5; HRMS (ESI, m/z) calculated for $C_{32}H_{43}N_2O_3$ $[M+H]^+$: 503.3274; found: 503.3288.

Ethyl (4R,4aS,6aR,9S,11aR,11bS,E)-4,9,11b-trimethyl-8-((((E)-3-(4-nitrophenyl)allyl)oxy)imino)tetradecahydro-6a,9-methanocyclohepta[a]naphthalene-4-carboxylate (6rf). White powder (403.7 mg, 77%); IR (KBr): 3020, 2927, 2849, 1721, 1519, 1452, 1344, 1223, 1026 cm^{-1}; ^1H NMR (400 MHz, $CDCl_3$): δ 8.19 (d, J = 8.8 Hz, 2H), 7.53 (d, J = 8.8 Hz, 2H), 6.67 (d, J = 16.1 Hz, 1H), 6.56 (dt, J = 5.4, 16.1 Hz, 1H), 4.75 (d, J = 5.4 Hz, 2H), 4.10 (m, 2H), 2.96 (dd, J = 3.1, 18.6 Hz, 1H), 2.19 (d, J = 13.3 Hz, 1H), 1.98 (d, J = 18.6 Hz, 1H), 1.58−1.91 (m, 8H), 1.40−1.49 (m, 4H), 1.28 (t, J = 7.2 Hz, 3H), 1.21−1.25 (m, 1H), 1.19 (s, 3H), 1.12 (s, 3H), 0.84−1.10 (m, 4H), 0.79 (s, 3H); ^{13}C NMR (100 MHz, $CDCl_3$): δ 177.4, 170.2, 146.9, 143.5, 131.5, 129.6, 127.0 (2C), 124.0 (2C), 73.4, 60.0, 57.2, 56.4, 54.9, 43.9, 43.7, 40.9, 40.7, 40.0, 39.6, 38.1, 38.0, 37.6, 29.0, 22.3, 21.7, 20.5, 19.0, 14.1, 13.5; HRMS (ESI, m/z) calculated for $C_{31}H_{43}N_2O_5$ $[M+H]^+$: 523.3172; found: 523.3173.

Ethyl (4R,4aS,6aR,9S,11aR,11bS,E)-4,9,11b-trimethyl-8-((((E)-3-(3,4,5-trifluorophenyl)allyl)oxy)imino)tetradecahydro-6a,9-methanocyclohepta[a]naphthalene-4-carboxylate (6rg). Pale yellow oil (441.5 mg, 83%); IR (KBr): 3020, 2929, 2848, 1721, 1614, 1529, 1441, 1346, 1234, 1042, 789 cm^{-1}; ^1H NMR (400 MHz, $CDCl_3$): δ 6.98 (m, 2H), 6.45 (d, J = 16.0 Hz, 1H), 6.30 (dt, J = 16.0, 5.6 Hz, 1H), 4.68 (d, J = 5.6 Hz, 2H), 4.09 (m, 2H), 2.93 (dd, J = 18.6, 3.1 Hz, 1H), 2.17 (d, J = 13.3 Hz, 1H), 1.95 (d, J = 18.6 Hz, 1H), 1.89−1.56 (m, 7H), 1.48−1.37 (m, 4H), 1.27 (t, J = 7.1 Hz, 3H), 1.24−1.19 (m, 2H), 1.18 (s, 3H), 1.10 (s, 3H), 1.07−0.83 (m, 4H), 0.77 (s, 3H); ^{13}C NMR (100 MHz, $CDCl_3$): δ 177.3, 170.0, 151.3 (ddd, J = 247.8, 10.1, 4.1 Hz), 138.9 (dt, J = 250.4, 15.3 Hz, 2C), 133.3, 129.1, 129.0, 110.2 (dd, J = 15.7, 5.7 Hz, 2C), 73.3, 59.9, 57.2, 56.4, 54.9, 43.8, 43.7, 40.9, 40.7, 40.0, 39.6, 38.1, 38.0, 37.6, 28.9, 22.2, 21.7, 20.4, 19.0, 14.1, 13.4; ^{19}F NMR (376.3 MHz, $CDCl_3$): δ −134.7, −161.8; HRMS (ESI, m/z) calculated for $C_{31}H_{41}F_3NO_3$ $[M+H]^+$: 532.3039; found: 532.3033.

Ethyl (4R,4aS,6aR,9S,11aR,11bS,E)-8-((((E)-3-(4-acetylphenyl) allyl)oxy)imino)-4,9,11b-trimethyltetradecahydro-6a,9-methanocyclohepta[a]naphthalene-4-carboxylate (6rh). White powder (390.5 mg, 75%); IR (KBr): 3020, 2933, 2848, 1719, 1683, 1603, 1453, 1360, 1233, 1028 cm^{-1}; ^1H NMR (400 MHz, $CDCl_3$): δ 7.91 (d, J = 8.3 Hz, 2H), 7.47 (d, J = 8.3 Hz, 2H), 6.64 (d, J = 16.0 Hz, 1H), 6.50 (dt, J = 5.7, 16.0 Hz, 1H), 4.73 (d, J = 5.7 Hz, 2H), 4.09 (m, 2H), 2.94 (dd, J = 2.9, 18.6 Hz, 1H), 2.59 (s, 3H), 2.17 (d, J = 13.2 Hz, 1H), 1.97 (d, J = 18.6 Hz, 1H), 1.56−1.90 (m, 8H), 1.38−1.48 (m, 4H), 1.26 (t, J = 7.1 Hz, 3H), 1.20−1.23 (m, 1H), 1.18 (s, 3H), 1.11 (s, 3H), 0.81−1.08 (m, 4H), 0.77 (s, 3H); ^{13}C NMR (100 MHz, $CDCl_3$): δ 197.6, 177.4, 170.0, 141.6, 136.0, 130.9, 129.4, 128.7 (2C), 126.5 (2C), 73.7, 60.0, 57.1, 56.5, 54.9, 43.8, 43.7, 40.9, 40.7, 40.0, 39.6, 38.1, 38.0, 37.6, 28.9, 26.6, 22.3, 21.7, 20.5, 19.0, 14.2, 13.5; HRMS (ESI, m/z) calculated for $C_{33}H_{46}NO_4$ $[M+H]^+$: 520.3427; found: 520.3433.

Ethyl (4R,4aS,6aR,9S,11aR,11bS,E)-4,9,11b-trimethyl-8-((((E)-3-(4-(oxazol-5-yl)phenyl)allyl)oxy)imino)tetradecahydro-6a,9-methanocyclohepta[a]naphthalene-4-carboxylate (6ri). White powder (398.4 mg, 73%); IR (KBr): 3127, 2930, 2848, 1719, 1606,

1453, 1363, 1219, 1029 cm^{-1}; ^1H NMR (400 MHz, $CDCl_3$): δ 7.85 (s, 1H), 7.52 (d, J = 8.3 Hz, 2H), 7.37 (d, J = 8.3 Hz, 2H), 6.54 (d, J = 16.0 Hz, 1H), 6.36 (dt, J = 5.9, 16.0 Hz, 1H), 4.67 (d, J = 5.9 Hz, 2H), 4.03 (m, 2H), 2.90 (dd, J = 2.8, 18.6 Hz, 1H), 2.11 (d, J = 13.2 Hz, 1H), 1.92 (d, J = 18.6 Hz, 1H), 1.50–1.82 (m, 7H), 1.31–1.41 (m, 4H), 1.21–1.27 (m, 1H), 1.19 (t, J = 7.2 Hz, 3H), 1.12–1.17 (m, 1H), 1.11 (s, 3H), 1.07 (s, 3H), 0.75–1.03 (m, 5H), 0.71 (s, 3H); ^{13}C NMR (100 MHz, $CDCl_3$): δ 177.2, 169.6, 151.3, 150.4, 137.2, 131.4, 127.1, 127.0 (2C), 126.7, 124.5 (2C), 121.5, 73.9, 59.9, 57.1, 56.4, 54.9, 43.8, 43.6, 40.9, 40.6, 39.9, 39.6, 38.0, 38.0, 37.6, 28.9, 22.3, 21.7, 20.4, 18.9, 14.1, 13.4; HRMS (ESI, m/z) calculated for $C_{34}H_{45}N_2O_4$ $[M+H]^+$: 545.3379; found: 545.3365.

Ethyl (4R,4aS,6aR,9S,11aR,11bS,E)-4,9,11b-trimethyl-8-((((E)-3-(4-(morpholinomethyl)phenyl)allyl)oxy)imino)tetradecahydro-6a,9-methanocyclohepta[a]naphthalene-4-carboxylate (6rj). Colourless oil (411.5 mg, 71%); IR (KBr): 3020, 2926, 2848, 1719, 1608, 1454, 1362, 1218, 1030 cm^{-1}; ^1H NMR (400 MHz, $CDCl_3$): δ 7.36 (d, J = 8.0 Hz, 2H), 7.29 (d, J = 8.0 Hz, 2H), 6.60 (d, J = 15.9 Hz, 1H), 6.37 (dt, J = 6.0, 15.9 Hz, 1H), 4.70 (d, J = 6.0 Hz, 2H), 4.10 (m, 2H), 3.71 (t, J = 4.6 Hz, 4H), 3.49 (s, 2H), 2.94 (dd, J = 2.9, 18.6 Hz, 1H), 2.45 (t, J = 4.6 Hz, 4H), 2.18 (d, J = 13.2 Hz, 1H), 1.96 (d, J = 18.6 Hz, 1H), 1.57–1.90 (m, 7H), 1.39–1.48 (m, 4H), 1.27 (t, J = 7.1 Hz, 3H), 1.20–1.24 (m, 1H), 1.18 (s, 3H), 1.12 (s, 3H), 0.84–1.08 (m, 5H), 0.77 (s, 3H); ^{13}C NMR (100 MHz, $CDCl_3$): δ 177.4, 169.7, 137.1, 136.0, 132.1, 129.4 (2C), 126.4 (2C), 125.9, 74.1, 67.0 (2C), 63.1, 60.0, 57.2, 56.5, 55.0, 53.6 (2C), 43.8, 43.7, 41.0, 40.7, 40.0, 39.6, 38.1, 38.0, 37.6, 28.9, 22.3, 21.7, 20.5, 19.0, 14.2, 13.4; HRMS (ESI, m/z) calculated for $C_{36}H_{53}N_2O_4$ $[M+H]^+$: 577.4005; found: 577.4014.

Ethyl (4R,4aS,6aR,9S,11aR,11bS,E)-8-((((E)-3-(1H-indol-5-yl)allyl)oxy)imino)-4,9,11b-trimethyltetradecahydro-6a,9-methanocyclohepta[a]naphthalene-4-carboxylate (6rk). Pale yellow powder (352.1 mg, 68%); IR (KBr): 3363, 3020, 2933, 2848, 1718, 1612, 1454, 1365, 1231, 1027 cm^{-1}; ^1H NMR (400 MHz, $CDCl_3$): δ 7.65 (s, 1H), 7.32–7.34 (m, 2H), 7.16–7.19 (m, 1H), 6.76 (d, J = 15.8 Hz, 1H), 6.52–6.55 (m, 1H), 6.36 (dt, J = 6.4, 15.8 Hz, 1H), 4.76 (d, J = 6.4 Hz, 2H), 4.12 (m, 2H), 2.99 (dd, J = 3.0, 18.6 Hz, 1H), 2.20 (d, J = 13.2 Hz, 1H), 2.02 (d, J = 18.6 Hz, 1H), 1.59–1.91 (m, 7H), 1.40–1.50 (m, 4H), 1.28 (t, J = 7.1 Hz, 3H), 1.22–1.25 (m, 1H), 1.21 (s, 3H), 1.16 (s, 3H), 0.84–1.13 (m, 5H), 0.80 (s, 3H); ^{13}C NMR (100 MHz, $CDCl_3$): δ 177.6, 169.7, 135.7, 134.2, 128.9, 128.1, 124.8, 122.9, 120.6, 119.4, 111.2, 102.8, 74.7, 60.1, 57.2, 56.5, 55.1, 43.8, 43.7, 41.0, 40.7, 40.0, 39.6, 38.1 (2C), 37.7, 29.0, 22.4, 21.7, 20.5, 19.0, 14.2, 13.4; HRMS (ESI, m/z) calculated for $C_{33}H_{45}N_2O_3$ $[M+H]^+$: 517.3430; found: 517.3441.

Ethyl (4R,4aS,6aR,9S,11aR,11bS,E)-8-((((E)-3-(benzofuran-5-yl)allyl)oxy)imino)-4,9,11b-trimethyltetradecahydro-6a,9-methanocyclohepta[a]naphthalene-4-carboxylate (6rl). White powder (332.1 mg, 64%); IR (KBr): 3020, 2927, 2848, 1719, 1609, 1467, 1364, 1234, 1030 cm^{-1}; ^1H NMR (400 MHz, $CDCl_3$): δ 7.59–7.63 (m, 2H), 7.37–7.47 (m, 2H), 6.75–6.76 (m, 1H), 6.72 (d, J = 16.1 Hz, 1H), 6.37 (dt, J = 6.2, 16.1 Hz, 1H), 4.74 (d, J = 6.2 Hz, 2H), 4.10 (m, 2H), 2.96 (dd, J = 3.0, 18.6 Hz, 1H), 2.18 (d, J = 13.2 Hz, 1H), 1.99 (d, J = 18.6 Hz, 1H), 1.59–1.88 (m, 7H), 1.39–1.49 (m, 4H), 1.27 (t, J = 7.1 Hz, 3H), 1.20–1.24 (m, 1H), 1.19 (s, 3H), 1.14 (s, 3H), 0.83–1.11 (m, 5H), 0.79 (s, 3H); ^{13}C NMR (100 MHz, $CDCl_3$): δ 177.4, 169.7, 154.7, 145.4, 132.8, 132.0, 127.7, 124.9, 123.0, 119.3, 111.4, 106.7, 74.3, 60.0, 57.2, 56.5, 55.0, 43.8, 43.7, 41.0, 40.7, 40.0, 39.6, 38.1, 38.0, 37.6, 28.9, 22.3, 21.7, 20.5, 19.0, 14.2, 13.4; HRMS (ESI, m/z) calculated for $C_{33}H_{44}NO_4$ $[M+H]^+$: 518.3270; found: 518.3279.

Ethyl (4R,4aS,6aR,9S,11aR,11bS,E)-8-((((E)-3-(benzo[b]thiophen-5-yl)allyl)oxy)imino)-4,9,11b-trimethyltetradecahydro-6a,9-methanocyclohepta[a]naphthalene-4-carboxylate (6rm). Pale yellow powder (66%); IR (KBr): 3043, 2927, 2848, 1719, 1655, 1452, 1363, 1230, 1152, 1029, 900 cm^{-1}; ^1H NMR (400 MHz, $CDCl_3$): δ 7.63–7.60 (m, 2H), 7.48–7.37 (m, 2H), 6.77–6.75 (m, 1H), 7.3 (d, J = 16.0 Hz, 1H), 6.38 (dt, J = 16.0, 6.2 Hz, 1H), 4.74 (d, J = 6.2 Hz, 2H), 4.10 (m, 2H), 2.96 (dd, J = 18.6, 3.0 Hz, 1H), 2.19 (d, J = 13.2 Hz, 1H), 1.99 (d, J = 18.6 Hz, 1H), 1.90–1.58 (m, 7H), 1.49–1.39 (m, 4H), 1.28 (t, J = 7.1 Hz, 3H), 1.25–1.21 (m, 1H), 1.19 (s, 3H), 1.14 (s, 3H), 1.12–0.84 (m, 5H), 0.79 (s, 3H); ^{13}C NMR (100 MHz, $CDCl_3$): δ 177.4, 169.7, 154.7, 145.4, 132.8, 132.0, 127.7, 124.9, 123.0, 119.3, 111.4, 106.7, 74.3, 60.0, 57.2, 56.5, 55.0, 43.8, 43.7, 40.9, 40.7, 40.0, 39.6, 38.1, 38.0, 37.6, 28.9, 22.3, 21.7, 20.5, 19.0, 14.2, 13.4; HRMS (ESI, m/z) calculated for $C_{33}H_{44}NO_3S$ $[M+H]^+$: 534.3042; found: 534.3036.

Ethyl (4R,4aS,6aR,9S,11aR,11bS,E)-4,9,11b-trimethyl-8-((((E)-3-(1-oxo-1,3-dihydroisobenzofuran-5-yl)allyl)oxy)imino)tetradecahydro-6a,9-methanocyclohepta[a]naphthalene-4-carboxylate (6rn). Colourless oil (325.8 mg, 61%); IR (KBr): 3020, 2934, 2848, 1768, 1716, 1616, 1453, 1352, 1232, 1042 cm^{-1}; ^1H NMR (400 MHz, $CDCl_3$): δ 7.75 (d, J = 8.0 Hz, 1H), 7.46 (d, J = 8.0 Hz, 1H), 7.42 (s, 1H), 6.62 (d, J = 16.1 Hz, 1H), 6.47 (dt, J = 5.5, 16.1 Hz, 1H), 5.23 (s, 2H), 4.66 (d, J = 5.5 Hz, 2H), 4.01 (m, 2H), 2.88 (dd, J = 2.4, 18.5 Hz, 1H), 2.09 (d, J = 13.2 Hz, 1H), 1.89 (d, J = 18.5 Hz, 1H), 1.49–1.83 (m, 7H), 1.30–1.42 (m, 4H), 1.19 (t, J = 7.1 Hz, 3H), 1.12–1.16 (m, 1H), 1.10 (s, 3H), 1.04 (s, 3H), 0.75–1.03 (m, 5H), 0.70 (s, 3H); ^{13}C NMR (100 MHz, $CDCl_3$): δ 177.2, 170.7, 169.9, 147.2, 143.0, 130.6, 130.4, 127.4, 125.7, 124.5, 119.6, 73.4, 69.4, 59.9, 57.1, 56.4, 54.8, 43.8, 43.6, 40.9, 40.6, 39.9, 39.5, 38.0, 37.9, 37.5, 28.9, 22.2, 21.6, 20.4, 18.9, 14.1, 13.4; HRMS (ESI, m/z) calculated for $C_{33}H_{44}NO_5$ $[M+H]^+$: 534.3219; found: 534.3228.

Ethyl (4R,4aS,6aR,9S,11aR,11bS,E)-8-((((E)-3-(dibenzo[b,d]furan-2-yl)allyl)oxy)imino)-4,9,11b-trimethyltetradecahydro-6a,9-methanocyclohepta[a]naphthalene-4-carboxylate (6ro). Colourless crystal (352.3 mg, 62%), m.p. 150.6–152.1 °C; X-ray crystal file is available from the Cambridge Crystallographic Data Centre: CCDC 1554566; IR (KBr): 3020, 2924, 2848, 1720, 1452, 1373, 1233, 1023 cm^{-1}; ^1H NMR (400 MHz, $CDCl_3$): δ 7.91–8.03 (m, 2H), 7.33–7.62 (m, 5H), 6.79 (d, J = 15.9 Hz, 1H), 6.45 (dt, J = 6.2, 15.9 Hz, 1H), 4.77 (d, J = 6.2 Hz, 2H), 4.11 (m, 2H), 2.98 (dd, J = 3.0, 18.6 Hz, 1H), 2.19 (d, J = 13.1 Hz, 1H), 2.01 (d, J = 18.7 Hz, 1H), 1.67–1.88 (m, 7H), 1.43–1.49 (m, 4H), 1.27–1.29 (m, 4H), 1.19 (s, 3H), 1.15 (s, 3H), 0.95–1.10 (m, 5H), 0.80 (s, 3H); ^{13}C NMR (100 MHz, $CDCl_3$): δ 177.4, 169.8, 156.6, 155.9, 132.5, 132.1, 127.3, 125.9, 125.3, 124.5, 124.1, 122.8, 120.7, 118.5, 111.7, 111.6, 74.3, 60.0, 57.2, 56.5, 55.0, 43.8, 43.7, 41.0, 40.7, 40.0, 39.6, 38.1, 38.0, 37.7, 28.9, 22.3, 21.7, 20.5, 19.0, 14.2, 13.5; HRMS (ESI, m/z) calculated for $C_{37}H_{46}NO_4$ $[M+H]^+$: 568.3427; found: 568.3432.

Ethyl (4R,4aS,6aR,9S,11aR,11bS,E)-8-((((E)-3-(9H-carbazol-3-yl)allyl)oxy)imino)-4,9,11b-trimethyltetradecahydro-6a,9-methanocyclohepta[a]naphthalene-4-carboxylate (6rp). Pale yellow powder (347.2 mg, 61%); IR (KBr): 3394, 2927, 2847, 1716, 1602, 1465, 1326, 1233, 1147, 1027, 753 cm^{-1}; ^1H NMR (400 MHz, $CDCl_3$): δ 8.4 (s, 1H), 8.1–8.06 (m, 2H), 7.53–7.23 (m, 5H), 6.82 (d, J = 15.8 Hz, 1H), 6.44 (dt, J = 15.8, 6.3 Hz), 4.82 (d, J = 6.3 Hz), 4.12 (m, 2H), 3.03 (dd, J = 18.6, 2.6 Hz, 1H), 2.21 (d, J = 13.2 Hz, 1H), 2.06 (d, J = 18.6, 1H), 1.94–1.60 (m, 7H), 1.54–1.40 (m, 4H), 1.28 (t, J = 7.1 Hz, 3H), 1.26–1.23 (m, 1H), 1.22 (s, 3H), 1.19 (s, 3H), 1.15–0.84 (m, 5H), 0.82 (s, 3H); ^{13}C NMR (100 MHz, $CDCl_3$): δ 177.6, 170.0, 140.0, 139.3, 133.9, 128.5, 125.9, 124.6, 123.5, 123.3, 123.1, 120.4, 119.5, 118.7, 110.8, 110.7, 74.7, 60.1, 57.2, 56.5, 55.0, 43.9, 43.8, 41.0, 40.7, 40.0, 39.6, 38.1, 38.0, 37.8, 29.0, 22.4, 21.8, 20.5, 19.0, 14.2, 13.5; HRMS (ESI, m/z) calculated for $C_{37}H_{47}N_2O_3$ $[M+H]^+$: 567.3587; found: 567.3583.

Methyl 4-((E)-3-((((4R,4aS,6aR,9S,11aR,11bS,E)-4-(ethoxycarbonyl)-4,9,11b-trimethyldodecahydro-6a,9-methanocyclohepta[a]naphthalen-8(7H)-ylidene)amino)oxy)prop-1-en-1-yl)-1H-pyrrole-2-carboxylate (6rq). Colourless oil (118.5 mg, 23%); IR (KBr): 3411, 3119, 2961, 2927, 2855, 1719, 1666, 1457, 1373, 1261, 1021 cm^{-1}; ^1H NMR (400 MHz, $CDCl_3$): δ 6.89–7.05 (m, 2H), 6.49 (d, J = 15.8 Hz, 1H), 6.13 (dt, J = 6.2, 15.8 Hz, 1H), 4.64

(d, $J = 6.2$ Hz, 2H), 4.10 (m, 2H), 3.87 (s, 3H), 2.87–2.98 (m, 1H), 2.18 (d, $J = 13.2$ Hz, 1H), 1.96 (d, $J = 18.7$ Hz, 1H), 1.60–1.87 (m, 7H), 1.38–1.48 (m, 4H), 1.27 (t, $J = 7.0$ Hz, 3H), 1.20–1.24 (m, 1H), 1.18 (s, 3H), 1.12 (s, 3H), 0.82–1.09 (m, 5H), 0.77 (s, 3H); ^{13}C NMR (100 MHz, $CDCl_3$): δ 177.5, 169.6, 161.5,125.2, 124.1, 123.5, 123.2, 121.3, 112.4, 74.4, 60.0, 57.2, 56.5, 55.0, 51.6, 43.8, 43.7, 41.0, 40.7, 40.0, 39.6, 38.1, 38.0, 37.6, 28.9, 22.3, 21.7, 20.5, 19.0, 14.2, 13.4; HRMS (ESI, m/z) calculated for $C_{31}H_{45}N_2O_5$ $[M-H]^-$: 523.3172; found: 523.3177.

Ethyl (4R,4aS,6aR,9S,11aR,11bS,E)-4,9,11b-trimethyl-8-((((E)-3-(naphthalen-1-yl)allyl)oxy)imino)tetradecahydro-6a,9-methanocyclohepta[a]naphthalene-4-carboxylate (6rr). Pale yellow powder (407.9 mg, 77%); IR (KBr): 3020, 2957, 2928, 2847, 1720, 1591, 1453, 1364, 1232, 1028 cm^{-1}; ^{1}H NMR (400 MHz, $CDCl_3$): δ 8.13–8.2 (m, 1H), 7.62–7.90 (m, 3H), 7.44–7.57 (m, 3H), 7.39 (d, $J = 15.7$ Hz, 1H), 6.43 (dt, $J = 5.8$, 15.7 Hz, 1H), 4.86 (d, $J = 5.8$ Hz, 2H), 4.11 (m, 2H), 3.03 (dd, $J = 3.0$, 18.6 Hz, 1H), 2.20 (d, $J = 13.3$ Hz, 1H), 2.04 (d, $J = 18.6$ Hz, 1H), 1.60–1.92 (m, 7H), 1.40–1.53 (m, 4H), 1.31–1.39 (m, 1H), 1.28 (t, $J = 7.2$ Hz, 3H), 1.21 (s, 3H), 1.19 (s, 3H), 0.84–1.13 (m, 5H), 0.81 (s, 3H); ^{13}C NMR (100 MHz, $CDCl_3$): δ 177.4, 169.8, 134.8, 133.6, 131.2, 129.6, 129.4, 128.5, 127.9, 126.0, 125.8, 125.6, 124.0, 123.9, 74.2, 60.0, 57.2, 56.5, 55.0, 43.9, 43.7, 41.0, 40.7, 40.0, 39.7, 38.1, 38.1, 37.7, 29.0, 22.4, 21.7, 20.5, 19.0, 14.2, 13.5; HRMS (ESI, m/z) calculated for $C_{35}H_{46}NO_3$ $[M+H]^+$: 528.3478; found: 528.3475.

Ethyl (4R,4aS,6aR,9S,11aR,11bS,E)-4,9,11b-trimethyl-8-((((E)-3-(quinolin-6-yl)allyl)oxy)imino)tetradecahydro-6a,9-methanocyclohepta[a]naphthalene-4-carboxylate (6rs). Pale yellow powder (345.0 mg, 65%); IR (KBr): 3020, 2949, 2931, 2847, 1718, 1590, 1453, 1379, 1230, 1026 cm^{-1}; ^{1}H NMR (400 MHz, $CDCl_3$): δ 8.81–8.87 (m, 1H), 8.01–8.12 (m, 2H), 7.81–7.86 (m, 1H), 7.66–7.69 (m, 1H), 7.32–7.38 (m, 1H), 6.76 (d, $J = 16.0$ Hz, 1H), 6.52 (dt, $J = 6.0$, 16.0 Hz, 1H), 4.75 (d, $J = 6.0$ Hz, 2H), 4.07 (m, 2H), 2.95 (dd, $J = 3.0$, 18.6 Hz, 1H), 2.15 (d, $J = 13.3$ Hz, 1H), 1.97 (d, $J = 18.6$ Hz, 1H), 1.58–1.83 (m, 7H), 1.38–1.45 (m, 4H), 1.24 (t, $J = 7.2$ Hz, 3H), 1.18–1.21 (m, 1H), 1.16 (s, 3H), 1.11 (s, 3H), 0.82–1.01 (m, 5H), 0.76 (s, 3H); ^{13}C NMR (100 MHz, $CDCl_3$): δ 177.3, 169.8, 150.0, 148.0, 136.0, 135.2, 131.4, 129.6, 128.4, 127.9, 127.4, 125.8, 121.4, 73.9, 59.9, 57.1, 56.5, 55.0, 43.8, 43.7, 40.9, 40.7, 39.9, 39.6, 38.0, 38.0, 37.6, 28.9, 22.3, 21.7, 20.5, 19.0, 14.1, 13.5; HRMS (ESI, m/z) calculated for $C_{34}H_{45}N_2O_3$ $[M+H]^+$: 529.3430; found: 529.3423.

Ethyl (4R,4aS,6aR,9S,11aR,11bS,E)-4,9,11b-trimethyl-8-((((E)-3-(quinoxalin-6-yl)allyl)oxy)imino)tetradecahydro-6a,9-methanocyclohepta[a]naphthalene-4-carboxylate (6rt). Brown powder (361.5 mg, 68%); IR (KBr): 2953.8, 2925.1, 2849.6, 1768.0, 1718.5, 1615.9, 1454.7, 1364.4, 1230.9, 1151.6, 1040.5, 892.1 cm^{-1}; ^{1}H NMR (400 MHz, $CDCl_3$): δ 8.75–8.65 (m, 2H), 7.98–7.77 (m, 3H), 6.73 (d, $J = 16.0$ Hz 1H), 6.54 (dt, $J = 16.0$, 5.7 Hz, 1H), 4.72 (d, $J = 5.7$ Hz, 2H), 4.01 (m, 2H), 2.90 (dd, $J = 18.5$, 2.9 Hz, 1H), 2.10 (d, $J = 13.2$ Hz, 1H), 1.92 (d, $J = 18.6$ Hz, 1H), 1.83–1.48 (m, 7H), 1.41–1.28 (m, 4H), 1.27–1.20 (m, 1H), 1.17 (t, $J = 7.1$ Hz, 3H), 1.15–1.12 (m, 1H), 1.09 (s, 3H), 1.05 (s, 3H), 1.02–0.73 (m, 4H), 0.71 (s, 3H); ^{13}C NMR (100 MHz, $CDCl_3$): δ 177.2, 169.7, 145.2, 144.4, 143.3, 142.7, 138.7, 130.7, 129.7, 129.4, 128.1, 126.9, 73.7, 59.9, 57.1, 56.4, 54.9, 43.8, 43.6, 40.9, 40.6, 39.9, 39.5, 38.0, 37.9, 37.5, 28.9, 22.3, 21.6, 20.4, 18.9, 14.1, 13.4; HRMS (ESI, m/z) calculated for $C_{33}H_{44}N_3O_3$ $[M+H]^+$: 530.3383; found: 530.3383.

Fragmentation characterization. Structural fragmentation characterization of the potent inhibitors was performed using ultrahigh-resolution tandem mass spectrometry [55–57]. Fragmentation characterization data of **6k** and **6p** with a suitable dissociation method are shown in Fig. 7. The characterization data of these compounds are presented in the Supporting Information. All mass spectra were collected in the positive ion mode using Fourier transform ion cyclotron resonance mass spectrometry (FT-ICR MS). A custom nanospray ion source was used to perform nano-electrospray ionization experiments. The samples were dissolved in 75:25 water/acetonitrile with 0.5% formic acid to a concentration of 5 μM. The capillary voltage was 900–1300 V, and the isolation window was 3 Da/e. The FT-ICR instrument was tuned to scan the m/z 147.4 to 3000 range. Ions were externally accumulated in the hexapole collision cell for 2 s before being transferred to the infinity cell for excitation and detection. Collision-induced dissociation (CID) experiments were performed using argon as the collision gas, the collision energy was optimized from 10 to 50 eV, and 18 eV and 30 eV were used for **6k** and **6p**, respectively. Electron-induced dissociation (EID) experiments were performed by irradiating the samples with electrons from a 1.5-A heated hollow cathode under an optimized bias voltage of 25 eV and a pulse length of 0.2 s. IRMPD experiments were carried out in the ICR cell by exposing the ions to a CO_2 laser beam (75 W and ~10.6 μm). The laser power was optimized to 50–60%, and the pulse duration was 0.5–0.6 s. All spectra were processed using Data Analysis software (Bruker Daltonik GmbH). The elemental compositions of most peaks were assigned with sub-ppm mass uncertainties using the Smart Formula function in Data Analysis.

Factor Xa Inhibition Assay. The compounds were tested for factor Xa inhibition using a chromogenic assay. The FXa assay was conducted in BSA buffer (0.05 M Tris, 0.1 M NaCl, 0.1% BSA, pH 7.4). Compounds were dissolved in dilute DMSO at concentrations from 100 μM to 1 nM and analyzed at a maximal final concentration of 0.1% unless otherwise stated. Assays were conducted in a 96-well microtiter plate with the control or test compound with both the buffer solution and the enzyme solution (human coagulation factor Xa from Kordia Human FXa). The reagents were mixed, centrifuged, and incubated for 15 min at 37 °C. The enzyme reaction was initiated by adding the substrate (for factor Xa, S-2765, Boatman Biotech, at a final concentration of 0.26 mM). The progress of the reaction was monitored for 1 h at 405 nm using a microtiter plate reader (Tecan M200). The inhibition rate was assessed using the formula [(OD/min) control - (OD/min) sample]/(OD/min) control. The IC_{50} was calculated using the inhibition rate from serial dilutions of the test compounds with SPSS19.0 software. To calculate the inhibition constant K_i [58], the IC_{50} value was corrected for competition with substrate using the formula calculated $K_i = IC_{50}/[1 + (\text{substrate concentration}/K_m)]$, the Michaelis constant K_m, for substrate hydrolysis by each protease was determined by fitting the data obtained from independent measurements at several substrate concentrations to the Michaelis–Menten equation.

Enzyme Affinity Assays. The serine proteases inhibition activities of compounds **6k** and **6p** were tested using a chromogenic assay. Human FXa was purchased from Kordia; human thrombin and FXIIa were purchased from American Diagnostica; human FIXa, FXIa and PK were purchased from Haematologic Technologies; human trypsin and chymotrypsin were purchased from Sigma Chemical; human FVIIa was purchased from Novo Pharmaceuticals; human tPA was purchased from Cloud-Clone Corp; human uPA was purchased from Molecular Innovations; rat FXa, rat thrombin, rat FIXa, rat tPA, and rat uPA were purchased from Molecular Innovations; rat FXIIa and rat trypsin were purchased from Abcam; rat FXIa, rat PK, and rat FVIIa were purchased from LifeSpan Biosciences; rat chymotrypsin was purchased from Abbexa; the FXa assay was conducted in BSA buffer (0.05 M Tris, 0.1 M NaCl, 0.1% BSA, pH 7.4). The factor XIa, factor XIIa, and chymotrypsin assays were conducted in 145 mM sodium chloride, 5 mM potassium chloride, 50 mM HEPES and 0.1% PEG 8000 at pH 7.4. The thrombin, trypsin, and plasma kallikrein assays were administered in 200 mM sodium chloride, 100 mM sodium phosphate, and 0.5% PEG 8000 at pH 7.5. The factor VIIa assays were performed in 150 mM sodium chloride, 5 mM calcium chloride, 50 mM HEPES, and 0.1% PEG 8000 at pH 7.4. The factor IXa assays were conducted in 100 mM

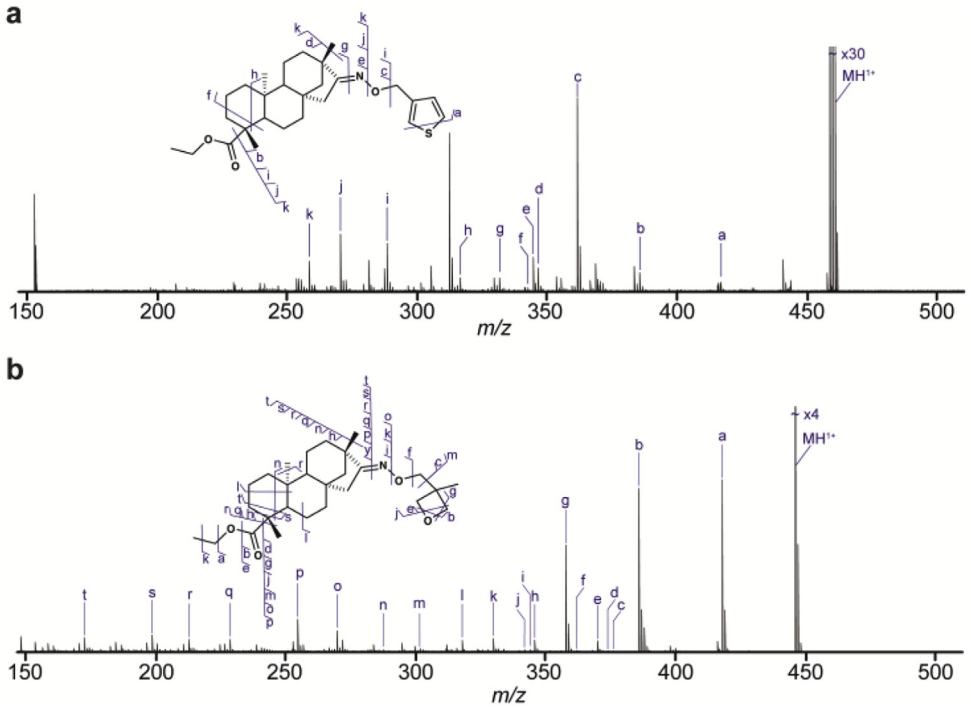

Fig. 7. Fragmentation characterization. (a) and (b) show the structural characterization of compounds **6k** and **6p**, respectively, using tandem mass spectrometry. The fragmentation methods used to obtain the spectra in (a) and (b) were electron-induced dissociation and infrared multiphoton dissociation, respectively.

sodium chloride, 5 mM calcium chloride, 50 mM Tris, 2% DMSO and 0.5% PEG 8000 at pH 7.4. The tPA and uPA assays were completed in 100 mM sodium chloride, 5 mM calcium chloride, 50 mM Tris, 2% DMSO and 0.5% PEG 8000 at pH 7.4.The peptide substrates were as follows: S-2765 (Boatman Biotech, for FXa, 0.26 mM), S-2222 (DiaPharma, for trypsin, 0.02 mM), S-2238 (DiaPharma, for thrombin, 0.007 mM), S-2302 (DiaPharma, for PK, 0.02 mM), S-2366 (DiaPharma, for FXIa, 0.73 mM), S-2288 (DiaPharma, for FVIIa, 5 mM), S-2586 (DiaPharma, for Chymotrypsin, 0.08 mM), Spectrozyme FIXa substrate (American Diagnostica Inc., for FIXa, 1.3 mM), Spectrozyme FXIIa substrate (American Diagnostica Inc., for FXIIa, 0.8 mM), Spectrozyme tPA substrate (Pentapharm, Aesch, Switzerland, 0.286 mM) and Spectrozyme uPA substrate (Pentapharm, Aesch, Switzerland, 82 mM). **6k** and **6p** were dissolved in dilute DMSO at concentrations from 100 μM to 1 nM and analyzed at a maximal final concentration of 0.1% unless otherwise noted. All assays were conducted in 96-well microtiter plates with control- or compound-containing buffer solutions and enzyme solution. The reagents were mixed, centrifuged, and then incubated for 15 min at 37 °C. The enzyme reaction was started by adding the substrate (All substrate concentrations used are equal to K_m values unless otherwise stated). The time course of the reaction was monitored at 405 nm in a microtiter plate reader (Tecan M200) for 1 h. The inhibition rate was measured from the formula, 1-[(OD/min) sample/(OD/min) control]. The IC_{50} was calculated using the inhibition rate of a dilution series of the compound with the SPSS19.0 software. To calculate the inhibition constant K_i, the IC_{50} value was corrected for competition with substrate using the formula calculated $K_i = IC_{50}/[1 + (\text{substrate concentration}/K_m)]$, the Michaelis constant K_m, for substrate hydrolysis by each protease was determined by fitting the data obtained from independent measurements at several substrate concentrations to the Michaelis–Menten equation.

Inhibition of ADP-induced Platelet Aggregation. One hour after receiving a 22 μmol/kg dose of the test compound or vehicle control solvent by oral gavage, the Wistar rats were anesthetized by intraperitoneal injection of 3% chloral hydrate (0.3 g/kg). Blood (4.5 mL) was extracted from the abdominal aorta and mixed with 3.8% sodium citrate solution (0.5 mL), and the mixture was centrifuged at 1200 rpm for 10 min at room temperature. After collecting the resulting platelet-rich plasma (PRP), the residue was centrifuged at 3000 rpm for another 10 min at room temperature to obtain the platelet-poor plasma (PPP). The PRP was adjusted with PPP to obtain a platelet count of $(30 \pm 5) \times 10^{10}$ Plts/L. The platelet aggregation test began with the addition of ADP (final concentration 10 μM) according to Born's method [59]. The results are expressed as the maximal aggregation rate within 5 min.

Docking Study. AutoDock Vina was used to predict the binding of the small molecules. We started from the coordinates 11.183, 4.941 and 22.323 and used a grid size of 12 Å. To analyze the docked structures, we manually visualized each docked pose for each molecule in PyMol (The PyMOL Molecular Graphics System, Version 1.8 Schrödinger, LLC). The criteria used to identify the model were good fit and good interactions, such as hydrogen bonds and interaction energies. The protein human factor Xa has been solved with different ligands. Although different ligands are present in the reported structures and they have different solved binding poses, the protein conformation remained stable. Thus, we used the protein as a rigid body and the known ligand binding site for docking our new compounds, **6k** and **6p**. **6k** and **6p** were docked in protein human factor Xa [PDBID: 2W26], and models for **6k** and **6p** that looked promising for ligand binding were found. The models for **6k** and **6p** both showed both good interactions and occupancy in the S1 and S4 pockets. The model for **6k** has a predicted binding affinity of −5.6 kcal/mol. The model for **6p** has a predicted binding affinity of −4.1 kcal/mol.

Pharmacokinetic Study. Pharmacokinetic studies of **6k** and **6p** were conducted on Wistar rats (210–230 g) with six rats (half male and half female) in each group. The test compounds were administered via oral gavage at 22 μmol/kg and via i.v. at 6.6 μmol/kg. Serial specimens (200 μL) were collected via the retrobulbar vein

(at 0.08, 0.17, 0.25, 0.5, 1, 2, 4, 6, 8, 12 and 24 h) and quantified by LC-MS/MS. LC-MS/MS analyses were performed on a UPLC system (LC-30AD, Shimadzu) with an Agilent ZORBAX Eclipse Plus C18 column (4.6 mm × 150 mm, 5 μm) and a triple quadrupole detector (API 4500, Turbospray source) using multiple-reaction monitoring (MRM) mode.

General Method for Pharmacology Study on Rats. Pharmacological studies (rats) of **6k** and **6p** were conducted on Wistar rats (210–230 g, half male and half female in each group) in accordance with the guidelines set by the NIH. Rivaroxaban, Clopidogrel, **6k** and **6p** were dissolved in distilled water at a concentration of 1 mg/mL with 0.104% (v/v) Tween-80. The vehicle control group was 0.104% (v/v) Tween-80 in distilled water at the same volume as was used in the experimental groups. The experiments were all conducted using oral gavage at a dosage of 22 μmol/kg. The animals were acclimatized for 3 days prior to the experiments.

Ex Vivo PT and aPTT Assays. The ex vivo PT and aPTT assays were conducted using the plasma of rats 1 h after administration of the test compound or vehicle control solvent at 22 μmol/kg by oral gavage, and the Wistar rats were anesthetized by intraperitoneal injection of 3% chloral hydrate (0.3 g/kg). Blood (4.5 mL) was extracted from the abdominal aorta, and then mixed with 3.2% sodium citrate (0.5 mL). PT and aPTT were detected using the corresponding blood coagulation assay kits according to the manufacturer's instructions and an automated coagulation analyzer.

Ex Vivo Thrombogenesis Model. The ex vivo antithrombotic efficacies were evaluated by observing the ex vivo thrombogenesis (wet weight and dry weight of thrombus) produced by the modified Chandler method. One hour after administration of the test compound or vehicle control solvent at 22 μmol/kg by oral gavage, the Wistar rats were anesthetized by intraperitoneal injection of 3% chloral hydrate (0.3 g/kg). Blood (3 mL) was extracted from the abdominal aorta, and then 1.8 mL of the blood was injected into the silicified thrombus tube. The two ends of the tube were joined to form a loop. The loop was placed on a rotating cylinder and rotated for 15 min, and then the wet weight of thrombus was measured by a precision torsion balance. After heating at 60 °C for 30 min, the dry weight of thrombus was measured in the same manner.

In Vivo Thrombogenesis Rats Model. The in vivo antithrombotic efficacies were evaluated by observing in vivo thrombogenesis (thrombus formation time) induced by stimulating the common carotid artery of rats with electricity. One hour after administration of the test compound or vehicle control solvent at 22 μmol/kg by oral gavage, the Wistar rats were anesthetized by intraperitoneal injection of 3% chloral hydrate (0.3 g/kg).The common carotid artery was carefully isolated, and a piece of parafilm was placed under the vessel to separate it from the surrounding tissue. The thrombus formation time was determined using an animal thrombus generator (YLS-14B, Yiyan-Tech, China). During the test, the stimulating electrode and temperature-controlled electrode were in full contact with the common carotid artery. The stimulation was initiated after the current had stabilized. The temperature of carotid blood abruptly decreases upon thrombus formation. The occlusion time was measured using the temperature sensor and timer on the electric thrombosis stimulator. The formation time was recorded as 30 min if the thrombus was not fully formed within 30 min.

Statistical Analysis. Graphs were plotted using GraphPad Prism 6 (GraphPad), and statistical analyses were performed using the same software unless otherwise stated. One-way ANOVA with Dunnett's post hoc analysis was used for multiple comparisons. Statistical significance is indicated as follows: $^{*}p < 0.05$, $^{**}p < 0.01$, $^{***}p < 0.001$, and $^{****}p < 0.0001$. Bar graphs depict the mean ± SD of independent experiments; each data point represents the measured value from an individual rat in the test group.

Associated content

Supporting **Information**. Detailed structural information of all the compounds; fragmentation characterization; in vitro FXa inhibitory activities of all the test compounds; detailed data from the enzyme inhibition assays; detailed data of the preliminary in vivo antithrombotic efficacies; detailed data from the coagulation assays; detailed data of the ex vivo and in vivo antithrombotic efficacies; NMR spectra; X-ray data.

Author contributions

P.C. designed and led the study under the supervision of H.F. P.C. designed the medicinal chemistry strategy and performed the organic chemistry and medicinal chemistry experiments. D.Z. and W.L. performed the pharmacokinetic study and the in vitro and in vivo pharmacology experiments. Q.W., Y.G. and C.C. performed in vitro enzyme inhibition experiments. M.L., P.Y.L. and P.B.O. designed and performed the mass spectrometry characterization experiments. N.B. and S.M. performed the docking study. P.C. wrote the manuscript, M.L. and P.B.O. revised the manuscript.

Notes

The authors declare no competing financial interests.

Acknowledgment

This research was supported by the National Natural Science Foundation of China (No. 81172943), the National Key Scientific and Technological Special Projects (No. 2012ZX09103201-022), and the Engineering and Physical Sciences Research Council (EP/F034210/1, EP/J000302/1, and EP/N021630/1).

Appendix A. Supplementary data

Supplementary data to this article can be found online at https://doi.org/10.1016/j.ejmech.2019.111722.

References

[1] M.G. Beckman, W.C. Hooper, S.E. Critchley, T.L. Ortel, Venous thromboembolism: a public health concern, Am. J. Prev. Med. 38 (2010) S495–S501.
[2] M.P. Turakhia, N.A. Estes 3rd, Stroke risk stratification in atrial fibrillation: bridging the evidence gaps, J. Cardiovasc. Electrophysiol. 27 (2016) 271–273.
[3] A.M. Wendelboe, G.E. Raskob, Global burden of thrombosis: epidemiologic aspects, Circ. Res. 118 (2016) 1340–1347.
[4] A. Schlitt, C. Jambor, M. Spannagl, W. Gogarten, T. Schilling, B. Zwissler, The perioperative management of treatment with anticoagulants and platelet aggregation inhibitors, Dtsch. Arztebl. Int. 110 (2013) 525–532.
[5] T.F. Luscher, J. Steffel, Individualized antithrombotic therapy, Hämostaseologie 36 (2016) 26–32.
[6] P.M. Bath, J. May, S. Heptinstall, Clinical utility of remote platelet function measurement using P-selectin: assessment of aspirin, clopidogrel, and prasugrel and bleeding disorders, Platelets 29 (2018) 425–430.
[7] J. Iwamoto, Y. Saito, A. Honda, Y. Matsuzaki, Clinical features of gastroduodenal injury associated with long-term low-dose aspirin therapy, World J. Gastroenterol. 19 (2013) 1673–1682.
[8] A. Zakarija, H.C. Kwaan, J.L. Moake, N. Bandarenko, D.K. Pandey, J.M. McKoy, P.R. Yarnold, D.W. Raisch, J.L. Winters, T.J. Raife, J.F. Cursio, T.H. Luu, E.A. Richey, M.J. Fisher, T.L. Ortel, M.S. Tallman, X.L. Zheng, M. Matsumoto, Y. Fujimura, C.L. Bennett, Ticlopidine- and clopidogrel-associated thrombotic thrombocytopenic purpura (TTP): review of clinical, laboratory, epidemiological, and pharmacovigilance findings, Kidney Int. Suppl (2009) S20–S24, 1989-2008.
[9] M. Levi, E.S. Eerenberg, P.W. Kampuisen, Anticoagulants. Old and new, Hämostaseologie 31 (2011) 229–235.
[10] C.M. Yu, A.A. Khattab, S.C. Bertog, A.P. Lee, J.S. Kwong, H. Sievert, B. Meier, Mechanical antithrombotic intervention by LAA occlusion in atrial fibrillation, Nat. Rev. Cardiol. 10 (2013) 707–722.
[11] R.H. van Gorp, L.J. Schurgers, New insights into the pros and cons of the clinical use of vitamin K antagonists (VKAs) versus direct oral anticoagulants

(DOACs), Nutrients 7 (2015) 9538–9557.
[12] A. Greinacher, T. Thiele, K. Selleng, Reversal of anticoagulants: an overview of current developments, Thromb. Haemost. 113 (2015) 931–942.
[13] J. Ansell, Factor Xa or thrombin: is factor Xa a better target? J. Thromb. Haemost. 5 (2007) 60–64.
[14] E. Perzborn, S. Roehrig, A. Straub, D. Kubitza, F. Misselwitz, The discovery and development of rivaroxaban, an oral, direct factor Xa inhibitor, Nat. Rev. Drug Discov. 10 (2011) 61–75.
[15] C. Frost, J. Wang, S. Nepal, A. Schuster, Y.C. Barrett, R. Mosqueda-Garcia, R.A. Reeves, F. LaCreta, Apixaban, an oral, direct factor Xa inhibitor: single dose safety, pharmacokinetics, pharmacodynamics and food effect in healthy subjects, Br. J. Clin. Pharmacol. 75 (2013) 476–487.
[16] D. Gretler, U. Sinha, M. Huo, M. Gent, W. Fisher, B. Davidson, K. Bauer, A. Turpie, A randomized evaluation of betrixaban, an oral factor Xa inhibitor, for prevention of thromboembolic events after total knee replacement (EXPERT), Thromb. Haemost. 101 (2017) 68–76.
[17] A. Plitt, R.P. Giugliano, Edoxaban: review of pharmacology and key phase I to III clinical trials, J. Cardiovasc. Pharmacol. Ther. 19 (2014) 409–416.
[18] J.H. Levy, A.C. Spyropoulos, C.M. Samama, J. Douketis, Direct oral anticoagulants: new drugs and new concepts, JACC Cardiovasc. Interv. 7 (2014) 1333–1351.
[19] J.L. Mega, E. Braunwald, S.D. Wiviott, J.-P. Bassand, D.L. Bhatt, C. Bode, P. Burton, M. Cohen, N. Cook-Bruns, K.A.A. Fox, S. Goto, S.A. Murphy, A.N. Plotnikov, D. Schneider, X. Sun, F.W.A. Verheugt, C.M. Gibson, Rivaroxaban in patients with a recent acute coronary syndrome, N. Engl. J. Med. 366 (2012) 9–19.
[20] J.H. Alexander, R.D. Lopes, S. James, R. Kilaru, Y. He, P. Mohan, D.L. Bhatt, S. Goodman, F.W. Verheugt, M. Flather, K. Huber, D. Liaw, S.E. Husted, J. Lopez-Sendon, R. De Caterina, P. Jansky, H. Darius, D. Vinereanu, J.H. Cornel, F. Cools, D. Atar, J.L. Leiva-Pons, M. Keltai, H. Ogawa, P. Pais, A. Parkhomenko, W. Ruzyllo, R. Diaz, H. White, M. Ruda, M. Geraldes, J. Lawrence, R.A. Harrington, L. Wallentin, Apixaban with antiplatelet therapy after acute coronary syndrome, N. Engl. J. Med. 365 (2011) 699–708.
[21] D.J.P. Pinto, J.M. Smallheer, D.L. Cheney, R.M. Knabb, R.R. Wexler, Factor Xa inhibitors: next-generation antithrombotic agents, J. Med. Chem. 53 (2010) 6243–6274.
[22] M. Iqbal, N.Y. Khalil, F. Imam, M. Khalid Anwer, A validated high-throughput UHPLC-MS/MS assay for accurate determination of rivaroxaban in plasma sample, J. Thromb. Thrombolysis 39 (2014) 79–88.
[23] S. Li, B. Liu, D. Xu, Y. Xu, Bleeding risk and mortality of edoxaban: a pooled meta-analysis of randomized controlled trials, PLoS One 9 (2014), e95354.
[24] N.C. Chan, V. Bhagirath, J.W. Eikelboom, Profile of betrixaban and its potential in the prevention and treatment of venous thromboembolism, Vasc. Health Risk Manag. 11 (2015) 343–351.
[25] M. de Candia, F. Liantonio, A. Carotti, R. De Cristofaro, C. Altomare, Fluorinated benzyloxyphenyl piperidine-4-carboxamides with dual function against thrombosis: inhibitors of factor Xa and platelet aggregation, J. Med. Chem. 52 (2009) 1018–1028.
[26] M. Correia-da-Silva, E. Sousa, B. Duarte, F. Marques, L.M. Cunha-Ribeiro, M.M. Pinto, Dual anticoagulant/antiplatelet persulfated small molecules, Eur. J. Med. Chem. 46 (2011) 2347–2358.
[27] M. Correia-da-Silva, E. Sousa, B. Duarte, F. Marques, F. Carvalho, L.M. Cunha-Ribeiro, M.M. Pinto, Polysulfated xanthones: multipathway development of a new generation of dual anticoagulant/antiplatelet agents, J. Med. Chem. 54 (2011) 5373–5384.
[28] Q. Rashid, M. Abid, N. Gupta, T. Tyagi, M.Z. Ashraf, M.A. Jairajpuri, Polysulfated trehalose as a novel anticoagulant agent with dual mode of action, BioMed Res. Int. 2015 (2015) 630482.
[29] W. Lee, H. Lee, M.A. Kim, J. Choi, K.M. Kim, J.S. Hwang, M. Na, J.S. Bae, Evaluation of novel factor Xa inhibitors from Oxya chinensis sinuosa with antiplatelet aggregation activity, Sci. Rep. 7 (2017) 7934.
[30] D. Hanjaya-Putra, C. Haller, X. Wang, E. Dai, B. Lim, L. Liu, P. Jaminet, J. Yao, A. Searle, T. Bonnard, C.E. Hagemeyer, K. Peter, E.L. Chaikof, Platelet-targeted dual pathway antithrombotic inhibits thrombosis with preserved hemostasis, JCI Insight (2018) 3.
[31] R. Morphy, Z. Rankovic, Designed multiple ligands. An emerging drug discovery paradigm, J. Med. Chem. 48 (2005) 6523–6543.
[32] J. Ilas, Z. Jakopin, T. Borstnar, M. Stegnar, D. Kikelj, 3,4-Dihydro-2H-1,4-benzoxazine derivatives combining thrombin inhibitory and glycoprotein IIb/IIIa receptor antagonistic activity as a novel class of antithrombotic compounds with dual function, J. Med. Chem. 51 (2008) 5617–5629.
[33] A.G. Atanasov, B. Waltenberger, E.M. Pferschy-Wenzig, T. Linder, C. Wawrosch, P. Uhrin, V. Temml, L. Wang, S. Schwaiger, E.H. Heiss, J.M. Rollinger, D. Schuster, J.M. Breuss, V. Bochkov, M.D. Mihovilovic, B. Kopp, R. Bauer, V.M. Dirsch, H. Stuppner, Discovery and resupply of pharmacologically active plant-derived natural products: a review, Biotechnol. Adv. 33 (2015) 1582–1614.
[34] K.C. Morrison, P.J. Hergenrother, Natural products as starting points for the synthesis of complex and diverse compounds, Nat. Prod. Rep. 31 (2014) 6–14.
[35] H. Lachance, S. Wetzel, K. Kumar, H. Waldmann, Charting, navigating, and populating natural product chemical space for drug discovery, J. Med. Chem. 55 (2012) 5989–6001.
[36] S. Patil, L.G. Lis, R.J. Schumacher, B.J. Norris, M.L. Morgan, R.A. Cuellar, B.R. Blazar, R. Suryanarayanan, V.J. Gurvich, G.I. Georg, Phosphonooxymethyl prodrug of triptolide: synthesis, physicochemical characterization, and efficacy in human colon adenocarcinoma and ovarian cancer xenografts, J. Med. Chem. 58 (2015) 9334–9344.
[37] A. Varadi, G.F. Marrone, T.C. Palmer, A. Narayan, M.R. Szabo, V. Le Rouzic, S.G. Grinnell, J.J. Subrath, E. Warner, S. Kalra, A. Hunkele, J. Pagirsky, S.O. Eans, J.M. Medina, J. Xu, Y.X. Pan, A. Borics, G.W. Pasternak, J.P. McLaughlin, S. Majumdar, Mitragynine/corynantheidine pseudoindoxyls as opioid analgesics with mu agonism and delta antagonism, which do not recruit beta-arrestin-2, J. Med. Chem. 59 (2016) 8381–8397.
[38] P. Schroder, J.O. Bauer, C. Strohmann, K. Kumar, H. Waldmann, Synthesis of an iridoid-inspired compound collection and discovery of autophagy inhibitors, J. Org. Chem. 81 (2016) 10242–10255.
[39] D. Harel, D. Schepmann, H. Prinz, R. Brun, T.J. Schmidt, B. Wunsch, Natural product derived antiprotozoal agents: synthesis, biological evaluation, and structure-activity relationships of novel chromene and chromane derivatives, J. Med. Chem. 56 (2013) 7442–7448.
[40] A.D. Kinghorn, D.D. Soejarto, N.P. Nanayakkara, C.M. Compadre, H.C. Makapugay, J.M. Hovanec-Brown, P.J. Medon, S.K. Kamath, A phytochemical screening procedure for sweet ent-kaurene glycosides in the genus Stevia, J. Nat. Prod. 47 (1984) 439–444.
[41] A. Roy, F.G. Roberts, P.R. Wilderman, K. Zhou, R.J. Peters, R.M. Coates, 16-Aza-ent-beyerane and 16-Aza-ent-trachylobane: potent mechanism-based inhibitors of recombinant ent-kaurene synthase from Arabidopsis thaliana, J. Am. Chem. Soc. 129 (2007) 12453–12460.
[42] J.P. Wang, H.X. Xu, Y.X. Wu, Y.J. Ye, J.L. Ruan, C.M. Xiong, Y.L. Cai, Ent-16beta,17-dihydroxy-kauran-19-oic acid, a kaurane diterpene acid from Siegesbeckia pubescens, presents antiplatelet and antithrombotic effects in rats, Phytomedicine 18 (2011) 873–878.
[43] W. Li, X. Tang, W. Yi, Q. Li, L. Ren, X. Liu, C. Chu, Y. Ozaki, J. Zhang, L. Zhu, Glaucocalyxin A inhibits platelet activation and thrombus formation preferentially via GPVI signaling pathway, PLoS One 8 (2013), e85120.
[44] M. Wang, H. Li, F. Xu, X. Gao, J. Li, S. Xu, D. Zhang, X. Wu, J. Xu, H. Hua, D. Li, Diterpenoid lead stevioside and its hydrolysis products steviol and isosteviol: biological activity and structural modification, Eur. J. Med. Chem. 156 (2018) 885–906.
[45] Y. Wu, J.H. Yang, G.F. Dai, C.J. Liu, G.Q. Tian, W.Y. Ma, J.C. Tao, Stereoselective synthesis of bioactive isosteviol derivatives as alpha-glucosidase inhibitors, Bioorg. Med. Chem. 17 (2009) 1464–1473.
[46] S.F. Chang, B.H. Chou, L.M. Yang, F.L. Hsu, W.K. Lin, Y. Ho, S.J. Lin, Microbial transformation of isosteviol oxime and the inhibitory effects on NF-kappaB and AP-1 activation in LPS-stimulated macrophages, Bioorg. Med. Chem. 17 (2009) 6348–6353.
[47] S.L. Zhu, Y. Wu, C.J. Liu, C.Y. Wei, J.C. Tao, H.M. Liu, Design and stereoselective synthesis of novel isosteviol-fused pyrazolines and pyrazoles as potential anticancer agents, Eur. J. Med. Chem. 65 (2013) 70–82.
[48] S.M. Bauer, E.A. Goldman, W. Huang, T. Su, L. Wang, J. Woolfrey, Y. Wu, J.F. Zuckett, A. Arfsten, B. Huang, J. Kothule, J. Lin, B. May, U. Sinha, P.W. Wong, A. Hutchaleelaha, R.M. Scarborough, B.Y. Zhu, Parallel synthesis and structure-activity relationships of a series of highly potent, selective, and neutral factor Xa inhibitors, Bioorg. Med. Chem. Lett 14 (2004) 4045–4050.
[49] Z. Huang, C. Velazquez, K. Abdellatif, M. Chowdhury, S. Jain, J. Reisz, J. Dumond, S.B. King, E. Knaus, Acyclic triaryl olefins possessing a sulfohydroxamic acid pharmacophore: synthesis, nitric oxide/nitroxyl release, cyclooxygenase inhibition, and anti-inflammatory studies, Org. Biomol. Chem. 8 (2010) 4124–4130.
[50] E. Abele, R. Abele, E. Lukevics, Oximes of five-membered heterocyclic compounds with three and four heteroatoms. Part 2. Synthesis of derivatives, reactions, and biological activity, Chem. Heterocycl. Comp. 44 (2008) 769–792.
[51] O. Trott, A.J. Olson, AutoDock Vina, Improving the speed and accuracy of docking with a new scoring function, efficient optimization, and multithreading, J. Comput. Chem. 31 (2010) 455–461.
[52] A.K. Jacobson, Platelet ADP receptor antagonists: ticlopidine and clopidogrel, Best Pract. Res. Clin. Haematol. 17 (2004) 55–64.
[53] J. Schneider, S. Wnendt, D. Saunders, R. Heinzel-Wieland, B. Wilffert, G. Steffens, Thrombin inhibitory and clot-specific fibrinolytic activities of the urokinase variant, M23 (rscu-PA-40 kDa/Hir), Eur. J. Pharmacol. 302 (1996) 69–77.
[54] B. Kalaska, E. Sokolowska, K. Kaminski, K. Szczubialka, K. Kramkowski, A. Mogielnicki, M. Nowakowska, W. Buczko, Cationic derivative of dextran reverses anticoagulant activity of unfractionated heparin in animal models of arterial and venous thrombosis, Eur. J. Pharmacol. 686 (2012) 81–89.
[55] J. Wei, H. Li, M.P. Barrow, P.B. O'Connor, Structural characterization of chlorophyll-a by high resolution tandem mass spectrometry, J. Am. Soc. Mass Spectrom. 24 (2013) 753–760.
[56] R.H. Wills, M. Tosin, P.B. O'Connor, Structural characterization of polyketides using high mass accuracy tandem mass spectrometry, Anal. Chem. 84 (2012) 8863–8870.
[57] J. Wei, P.B. O'Connor, Extensive fragmentation of pheophytin-a by infrared multiphoton dissociation tandem mass spectrometry, Rapid Commun. Mass Spectrom. 29 (2015) 2411–2418.
[58] Y.-C. Cheng, W.H. Prusoff, Relation between the inhibition constant K1) and the concentration of inhibitor which causes fifty per cent inhibition (I50) of an enzymic reaction, Biochem. Pharmacol. 22 (1973) 3099–3108.
[59] G.V. Born, Aggregation of blood platelets by adenosine diphosphate and its reversal, Nature 194 (1962) 927–929.